Annu. Rev. Astron. Astrophys. 1998. 36:599–654

SIMULATIONS OF STRUCTURE FORMATION IN THE UNIVERSE

Edmund Bertschinger
Department of Physics, Massachusetts Institute of Technology, 77 Massachusetts Avenue, Room 6-207, Cambridge, Massachussetts 02139; email: edbert@mit.edu

KEY WORDS: cosmology, galaxy formation, numerical simulation

ABSTRACT

Cosmic structure has formed as a result of gravitational amplification of primordial density fluctuations together with the action of other physical processes (adiabatic gas dynamics, radiative cooling, photoionization and recombination, radiative transfer). These complex nonlinear processes, acting over a wide range of length scales (from kiloparsecs to tens of megaparsecs), make this a difficult problem for computation. During the last two decades, significant progress has been made in developing numerical methods and statistical tools for analyzing simulations and data. Combined with observational advances, numerical simulations have led to the demise of several formerly popular models and to an improved understanding of galaxy clusters, quasistellar object (QSO) absorption line systems, and other phenomena. This review summarizes these advances.

1. INTRODUCTION

During the past twenty years, numerical simulations of cosmic structure formation have become a powerful theoretical tool to accompany, interpret, and sometimes to lead cosmological observations. Simulations bridge the gap that often exists between basic theory and observation. They have found many uses, including testing and calibrating methods used to measure cosmological parameters, providing insight into nonlinear gravitational clustering and hydrodynamic turbulence, helping to explain the nature of systems such as quasistellar object (QSO) absorption lines, and highlighting shortcomings in the current physical modeling of galaxy formation. However, their main use has been and continues to be testing the viability of cosmological models

0066-4146/98/0915-0599$08.00

of structure formation, such as the cold dark matter (CDM) model and its variants.

Structure formation models attempt to reduce cosmology to an initial value problem. Given the initial conditions—a background cosmological model with specified composition of matter, radiation, and exotic fields, such as a cosmological constant, and primordial fluctuations in the matter, radiation, and spacetime geometry—the goal is to compute using well-known laws of physics the evolution of structure from the Big Bang to the present day. At any useful level of abstraction, the Universe is an exceedingly complex system, hence analytic theory has only a limited (but nonetheless valuable) place in cosmic structure formation.

The current generation of cosmological simulations has antecedents that date back several decades. The first gravitational *N*-body simulation of interacting galaxies was performed using an analog optical computer (Holmberg 1941): Gravity was represented by the flux from 37 lightbulbs, with photocells and galvanometers used to measure and display the inverse square law force. The first astronomical *N*-body computations using digital computers were made in the early 1960s (von Hoerner 1960, 1963, Aarseth 1963). These early simulations were limited to at most about 100 particles. Gas dynamical simulations of galaxy formation began with the pioneering spherically symmetric calculations of Larson (1969). Increasingly large simulations of cluster collapse and evolution were performed throughout the 1970s (e.g. Peebles 1970, White 1976).

The first truly cosmological simulations of structure formation were the *N*-body integrations of Press & Schechter (1974) in their influential paper on the mass distribution of bound clumps formed by hierarchical clustering. At almost the same time, smaller simulations of cosmological clustering were performed by Haggerty & Janin (1974). This work was followed by numerous studies of the evolution of the two-point correlation function, a measure of galaxy clustering (Miyoshi & Kihara 1975, Groth & Peebles 1976, Fall 1978, Aarseth et al 1979, Efstathiou 1979, Gott et al 1979). Early work on galaxy formation was reviewed by Gott (1977).

The early 1980s saw several important developments leading to an explosion of activity in simulations of cosmic structure formation:

1. Plausible physical models for dark matter had been proposed (Cowsik & McClelland 1972, Lee & Weinberg 1977, Bond et al 1980), including massive neutrinos (also known as hot dark matter or HDM) and cold dark matter (CDM; see Trimble 1987 for a review of dark matter).

2. Cosmic inflation (Guth 1981) was shown to produce naturally the scale-invariant Harrison-Zel'dovich spectrum (Harrison 1970, Zel'dovich 1972) of primordial fluctuations in matter and radiation (Guth & Pi 1985 and

references therein). In $\Omega = 1$ (critical density) models, the initial conditions were thus reduced to specification of one number (the fluctuation amplitude) plus the composition of matter and radiation.

3. Accurate numerical computations were made of the evolution of density fluctuations from their generation in the early Universe through recombination to the onset of nonlinear evolution (Peebles & Yu 1970, Bond & Szalay 1983).

3. The theory of Gaussian random fields was developed and applied to the statistics of primordial density fields (Doroshkevich 1970, Bardeen et al 1986). Methods were developed to simulate Gaussian random fields with arbitrary power spectra (Efstathiou et al 1985, Peacock & Heavens 1985), using the Zel'dovich (1970) approximation to produce only the growing mode (Doroshkevich et al 1980, Dekel 1982).

4. Grid-based *N*-body algorithms were applied to cosmology, enabling dark matter simulations with more than 10^5 particles to be performed (Section 2.1 below).

With all these developments occurring within a few years, there was great optimism among many working in this area that cosmologists were on the verge of understanding the formation of large-scale structure in the Universe. The CDM model became the paradigm of this new understanding (Peebles 1982, Blumenthal et al 1984, Davis et al 1985).

As interest in structure formation grew during the 1980s, increasingly sophisticated tests were made of the CDM model. Problems began to appear, with the model seeming to show too little clustering on large ($\sim 50\ h^{-1}$ Mpc, $h = H_0/100$ km s^{-1} Mpc^{-1}) scales compared with the real Universe when normalized to produce the correct amplitude on galaxy and cluster scales (see Ostriker 1993 for a review). The long sought after measurement of anisotropy in the cosmic microwave background radiation (Smoot et al 1992) highlighted and recast this problem: The CDM model has excessive power on small scales when normalized to produce the measured microwave background anisotropy (Efstathiou et al 1992). Although the optimism of the early 1980s waned, it was replaced by an appreciation that structure formation is a richer problem that needs the incorporation of much more physics into cosmological simulations, especially of gas dynamics for the ordinary ("baryonic") matter that is all we can see directly.

With the demise of the simplest detailed model of structure formation, attention has turned to variants that retain many of the attractive features of the CDM model while attempting to repair its deficiencies. These include replacing some

of the CDM with light massive neutrinos (i.e. with HDM) or a cosmological constant; tilting the primordial spectrum; or including spatial curvature. Another class of models has the fluctuations seeded from topological defects like cosmic strings or global textures (Brandenberger 1994, Vilenkin & Shellard 1994) instead of quantum fluctuations produced during inflation. Texture models now appear to be inconsistent with the measured anisotropy of the cosmic microwave background (Pen et al 1997).

The last decade has seen an impressive growth not only in the size of cosmological simulations—hydrodynamic grids of 512^3 with 16 million or more particles tracing the dark matter are now almost common—but also in the sophistication of the physics. Although baryons are thought to contribute anywhere from about 3–30% of the total mass in the Universe (depending on the uncertain value of Ω, the mean density of nonrelativistic matter in units of the critical density), they are responsible for 100% of the light we see, and they dominate the mass of the bulges and disks of galaxies. Cosmological gas dynamics has now come into maturity with a variety of algorithms being applied and compared with each other and with observations (e.g. Kang et al 1994).

This article reviews the techniques and results of cosmological structure formation simulations since the early 1980s. For the purposes of this article, cosmological simulations begin, by definition, with small-amplitude stochastic fluctuations in an expanding universe generated at high redshift. No attempt is made to review simulations of galaxies, galaxy groups, or clusters treated in isolation without such initial conditions. Only a limited discussion space is given to simulations of topological defects, computations of primary microwave background anisotropy (see White et al 1994 and Bond 1996 for pedagogical reviews), analytic and semianalytic models of galaxy formation (White 1996), and simulations based on approximate quasilinear dynamics. While many simulations have been devoted to large-scale structure, that subject has been reviewed recently elsewhere (Dekel 1994, Strauss & Willick 1995, Efstathiou 1996) and no attempt is made at a comprehensive summary here. Sections 2 and 3, summarizing simulation and analysis methods, present technical matter of interest primarily to experts. Others may wish to skip directly to Section 4.

As this article was prepared, a bibliography of approximately 900 refereed articles relevant to cosmological simulations was compiled. This bibliography is available on the World Wide Web in the Supplemental Materials Section of the Annual Reviews site (http://www.AnnualReviews.org).

2. SIMULATION ALGORITHMS

Cosmological simulations incorporate a range of physics: gravitation, gas dynamics (adiabatic or with radiative cooling and heating), chemistry, and

radiative transfer. The first is obligatory and the rest are important, even necessary, refinements. These computations are nearly always performed using comoving spatial coordinates and periodic boundary conditions so that a finite, expanding volume is embedded in an appropriately perturbed background spacetime.

2.1 *Gravity Calculation and Dark Matter Evolution*

Dark matter is represented in cosmological simulations by particles sampling the phase space distribution. Particles are evolved forward in time using Newton's laws written in comoving coordinates (Peebles 1980):

$$\frac{d\vec{x}}{dt} = \frac{1}{a}\vec{v}, \quad \frac{d\vec{v}}{dt} + H\vec{v} = \vec{g}, \quad \vec{\nabla}\cdot\vec{g} = -4\pi G a[\rho(\vec{x},t) - \bar{\rho}(t)]. \tag{1}$$

Here $a(t)$ is the cosmic expansion factor (related to redshift z by $a^{-1} = 1+z$), $H = d\ln a/dt$ is the Hubble parameter, $\vec{v}$ is the peculiar velocity, ρ is the mass density, $\bar{\rho}$ is the spatial mean density, and $\vec{\nabla} = \partial/\partial\vec{x}$ is the gradient in comoving coordinates. Note that the first pair of relationships in Equation 1 is to be integrated for every dark matter particle by using the gravity field produced by all matter (dark and baryonic) contributing to ρ.

The time integration of particle trajectories is generally performed using a second-order accurate leapfrog integration scheme requiring only one force evaluation per timestep (Efstathiou et al 1985). While higher-order schemes would provide more accurate trajectories with longer timesteps, they are rarely used in cosmological simulations because of the costly requirement for calculating and storing additional forces or their derivatives. Mass resolution is generally considered more important than attempting to accurately follow individual particle trajectories, especially because the latter are chaotic (Goodman et al 1993 and references therein). The simulator aims to follow accurately the motions of gravitationally bound concentrations of hundreds or more particles while bearing in mind that the particles themselves are samples of the dark matter phase space.

In practice, it is preferable to use $s = \int a^{-2}\,dt$ as the time variable for cosmological N-body integrations instead of proper time because the equations of motion then simplify to $d^2\vec{x}/ds^2 = a\vec{g}$, which allows a symplectic (phase space–volume preserving) integrator for $\vec{x}$ and $d\vec{x}/ds$ (Quinn et al 1997). The simple leapfrog integrator is symplectic when used with an appropriately chosen timestep for these variables (Hut et al 1995). Another consideration is the use of individual timesteps (Hernquist & Katz 1989), which can significantly speed up highly clustered simulations if the force evaluation is not dominated by fixed costs that are independent of particle number.

The art of N-body simulation lies chiefly in the computational algorithm used to obtain the gravitational force. The desired pair force is a softened inverse

square law representing the force between two finite-size particles in order to prevent the formation of unphysical tight binaries. Evaluating the forces by direct summation over all particle pairs is prohibitive even with the largest parallel supercomputers. For $N = 10^7$, a typical number for present-day cosmological simulations, a single force evaluation by direct summation would take several hours on a 100-GFlops (1 GFlops $= 10^9$ floating point operations per second) machine but only a few seconds by fast algorithms. For collisional N-body systems like globular clusters, where greater accuracy is required, special-purpose processors like the GRAPE series (Makino et al 1997 and references therein) hold great promise. Recently a GRAPE-4 running at a sustained speed of 406 Gflops was used to simulate the formation of a single dark matter halo with high precision (Fukushige & Makino 1997). Even in large-scale cosmological simulations, when the force evaluation is separated into long-range and short-range parts, the GRAPE processor can be used effectively to speed up the computation of dense regions (Brieu et al 1995, Steinmetz 1996).

2.1.1 BARNES-HUT TREE ALGORITHM The hierarchical tree algorithm (Appel 1985, Barnes & Hut 1986) divides space recursively into a hierarchy of cells, each containing one or more particles. If a cell of size s and distance d (from the point where $\vec{g}$ is to be computed) satisfies $s/d < \theta$, the particles in this cell are treated as one pseudoparticle located at the center of mass of the cell. Computation is saved by replacing the set of particles by a low-order multipole expansion due to the distribution of mass in the cell.

The tree algorithm has a number of important advantages (Hernquist 1987, 1988, Barnes & Hut 1989, Jernigan & Porter 1989). Foremost is its speed: $O(N \log N)$ operations are required to compute all forces on N particles. Force errors can be bounded and made small by choosing $\theta < 1$ and including quadrupole and high-order moments to the inverse square law. It is also relatively easy to implement, and Barnes & Hut (1989) made their code publicly available, leading to its widespread use. Finally, the algorithm is fully spatially adaptive—the hierarchical tree automatically refines resolution where needed. One drawback is the relatively large amount of memory required, from $20N$ to $30N$ words for N particles (Hernquist 1987). Another complication is that the tree algorithm, like direct summation itself, does not provide periodic boundary conditions. However, this can be corrected using a procedure known as Ewald (1921) summation, leading to a practical tree code for cosmological applications (Bouchet & Hernquist 1988, Hernquist et al 1991).

Several groups have parallelized the tree algorithm (Hillis & Barnes 1987, Makino & Hut 1989, Olson & Dorbrand 1994, Salmon & Warren 1994, Dubinski 1996, Governato et al 1997), enabling cosmological large-scale structure simulations to be performed with more than 16 million particles (Zurek et al 1994, Brainerd et al 1996).

2.1.2 PARTICLE-MESH ALGORITHM The particle-mesh (PM) method is based on representing the gravitational potential on a Cartesian grid (with a total of N_g grid points), used in solving Poisson's equation on this grid. The development of the Fast Fourier Transform (FFT) algorithm (Cooley & Tukey 1965) made possible a fast Poisson solver requiring $O(N_g \log N_g)$ operations (Miller & Prendergast 1968, Hohl & Hockney 1969, Miller 1970). Periodic boundary conditions are automatic, making this algorithm natural for cosmology, and its simplicity has led to many independent implementations (in two dimensions by Doroshkevich et al 1980, Melott 1983, and Bouchet et al 1985, and subsequently in three dimensions by Centrella & Melott 1983, Klypin & Shandarin 1983, Miller 1983, White et al 1983, Bouchet & Kandrup 1985, and many others since). Hockney & Eastwood (1988) have written an excellent monograph on the PM and particle-particle/particle-mesh (P^3M) methods (the latter is discussed in Section 2.1.3 below).

The PM algorithm has three steps. The mass density field is first computed on a grid. Poisson's equation is then solved for the gravity field (or the potential, which is then differenced to give the gravity field). Finally, the gravity field on the grid is interpolated back to the particles.

The first step is called mass assignment: $\rho(\vec{x}, t)$ is computed on the grid from discrete particle positions and masses. The simplest method assigns each particle to the nearest grid point (NGP), with no contribution of mass to any other grid point. Unsurprisingly, this method produces rather large truncation errors (Efstathiou et al 1985, Hockney & Eastwood 1988). The most commonly used assignment scheme is Cloud-in-Cell (CIC), which uses multilinear interpolation to the eight grid points defining the cubical mesh cell containing the particle. This procedure effectively treats each particle as a uniform-density cubical cloud. The sharp edges introduce force fluctuations, which can be reduced by using a higher-order interpolation scheme (e.g. Triangular Shaped Cloud or TSC, which uses the nearest 27 grid points). These discretization errors are similar to aliasing errors that occur in image processing. They may be reduced further using a suitable anti-aliasing filter ("Quiet PM" of Hockney & Eastwood 1988; see also Ferrell & Bertschinger 1994).

The heart of the PM algorithm is the Fourier space solution of the Poisson equation for the gravitational potential:

$$\hat{\phi}(\vec{k}, t) = -4\pi G a^2 \frac{\hat{\rho}(\vec{k}, t)}{k^2}. \tag{2}$$

Here $\hat{\rho}$ and $\hat{\phi}$ are the discrete Fourier transforms of the mass density and potential, respectively. One may replace the inverse Laplacian operator $-1/k^2$ by another multiplicative factor in Fourier space, optionally including an anti-aliasing filter. The gravity field is then obtained by transforming the potential back to the spatial domain and approximating the gradient by finite differences,

or by multiplication by $i\vec{k}$ in the Fourier domain (with care taken when any wave vector component reaches the Nyquist frequency). The latter method requires twice as many FFTs but leads to slightly more accurate forces (Ferrell & Bertschinger 1994).

The third step is to interpolate the gravity from the grid back to the particles. The same interpolation scheme should be used here as in the first step (mass assignment) to ensure that self-forces on particles vanish (Hockney & Eastwood 1988).

The PM method has the advantage of speed, requiring $O(N) + O(N_g \log N_g)$ operations to evaluate the forces on all particles. For typical grid sizes (with twice as many grid points as particles in each dimension), it requires less memory and is faster per timestep than the tree algorithm. However, the forces approximate the inverse square law poorly for pair separations less than several grid spacings. Each particle has an effective diameter of about two grid spacings and a nonspherical shape (particle isotropy can be improved with an anti-aliasing filter at the expense of a larger particle diameter). Also, obtaining isolated instead of periodic boundary conditions (desirable for simulations of galaxies and galaxy groups, if not for cosmology) requires a factor of 8 increase in storage in three dimensions (Hohl & Hockney 1969), unless the complicated method of James (1977) is implemented. For high-resolution studies of galaxy dynamics, the tree code is generally considered much superior. PM codes are widely used for large-scale cosmological simulations. The PM algorithm has been parallelized by Ferrell & Bertschinger (1994).

2.1.3 P^{3}M AND ADAPTIVE P^{3}M The primary drawback of the particle-mesh method is that its force resolution (effectively, the particle size) is limited by the spatial grid. This limitation can be removed by supplementing the forces with a direct sum over pairs separated by less than two or three grid spacings, resulting in the particle-particle/particle-mesh (P^{3}M) algorithm. This hybrid algorithm, first developed for plasma physics by Hockney et al (1974), was applied in cosmology by Efstathiou & Eastwood (1981). It is described in detail by Hockney & Eastwood (1988) and Efstathiou et al (1985), and it was used extensively by the latter authors in a series of articles beginning with Davis et al (1985). Cosmological P^{3}M codes have also been developed by Bertschinger & Gelb (1991), Martel (1991), and others.

The P^{3}M method readily achieves high accuracy forces through the combination of mesh-based and direct summation forces. The mesh may be regarded as simply a convenience for providing periodic boundary conditions and removing much of the burden of computation from the direct pair summation. However, when clustering becomes strong, as occurs inevitably on small scales in realistic, high-resolution cosmological simulations, the cost of the direct summation

dominates, severely degrading the performance of P^3M. One solution is to replace the direct summation by a tree code (Xu 1995) or fast hardware (Brieu et al 1995, Fukushige et al 1996).

In his mesh-refined P^3M algorithm, Couchman (1991) presented an elegant solution to the bottleneck of strong clustering. Subgrids are placed over regions of high density to shift some of the burden of force evaluation away from pair summation and over to a subgrid PM calculation with isolated boundary conditions. Pair summation is still done, but only for pairs whose separation is less than two to three spacings of the subgrid mesh, resulting in a substantial reduction. Multiple levels of grid refinement may be used to further reduce pair summation in dense regions. The philosophy of this method is to compute the exact desired pair force, to within a fraction of a percent accuracy for (almost) every pair, by using the combination of mesh-based PM and pair summation that gives the optimal performance. Because the pair summation no longer dominates as it does in P^3M, the force computation of this new, adaptive P^3M scales as $O(N \log N)$, similar to a tree code but with a somewhat smaller coefficient (Bertschinger & Gelb 1991, Couchman 1991). An example of the refinement grids used for a strongly clustered simulation is shown in Figure 1.

The P^3M algorithm has been parallelized by Ferrell & Bertschinger (1994, 1995), by Theuns (1994), and, including adaptive refinement, by Pearce & Couchman (1997) as part of their HYDRA code, which also includes smooth-particle hydrodynamics. At the present time, parallel adaptive P^3M appears to be the method of choice for large cosmological N-body simulations.

2.1.4 MULTIRESOLUTION MESH METHODS Adaptive P^3M avoids the resolution limit imposed by a mesh by using a combination of finer meshes and pair summation. An alternative is to dispense with pair summation altogether, instead refining or concentrating the mesh where dictated by the needs of accuracy or speed. This may be done by placing one or more levels of mesh refinement where desired and solving the Poisson equation on multiple grids. Multiple resolution algorithms have long been used in computational fluid dynamics, but only recently have they been applied in cosmology. Here the programmer must decide whether to refine only the force resolution (similar to using a finer mesh in a PM simulation) or also to refine the mass resolution (equivalent to using more particles in selected regions).

Methods that refine force but not mass resolution are similar in spirit to adaptive P^3M in that they use a fixed set of (usually but not necessarily equal-mass) particles. Several groups have developed codes that automatically refine the spatial resolution where needed during the computation by using higher-resolution meshes (adaptive mesh refinement): Jessop et al (1994), Suisalu &

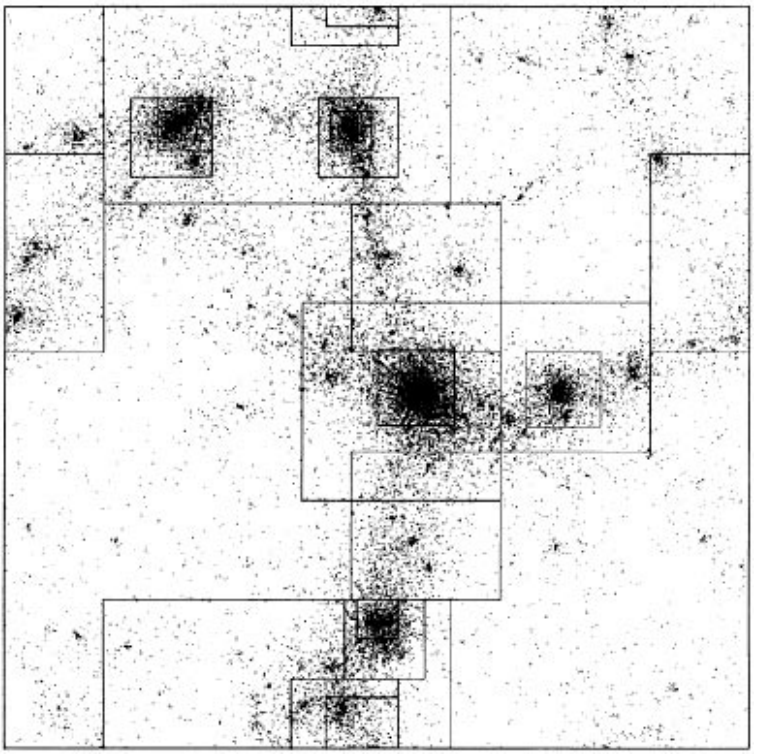

Figure 1 Distribution of grid refinements placed by an adaptive particle-particle/particle-mesh–smooth-particle hydrodynamics (P^3M-SPH) code for the final timestep of a cluster simulation. Gas particles are shown. From Couchman et al (1995).

Saar (1995), Gelato et al (1997), and Kravtsov et al (1997). Unlike P^3M, these codes have a variable spatial resolution of the forces. Although this leads to an effective particle size that changes as particles move across refinements, it may be closer to the spirit of phase space sampling with a resolution that might, for example, scale with the local mean particle spacing.

Another class of methods refines both the mass and force resolution by splitting particles into several lower-mass particles and using multiple grids for the force computation. All of these algorithms published to date are nonadaptive; they work with nested grids that are fixed in space. The first implementation was the hierarchical PM solver of Villumsen (1989). In Villumsen's method, an ordinary PM simulation is performed first to identify regions needing higher resolution. The simulation is then repeated with high-resolution meshes added. Particles that enter these regions (as judged by the first simulation) are split

into several lower-mass particles. High-frequency waves are added to their initial displacements and velocities to simultaneously increase the sampling of the initial power spectrum. Anninos et al (1994) and Dutta (1995) have implemented similar algorithms with some improvements; Dutta used a tree code for the high-resolution forces in place of PM. Splinter (1996) chose to split up massive particles only when they enter the refinement volume rather than at the beginning of the simulation. While this precludes refining the sampling of the initial power spectrum, it is less costly and closer to the spirit of adaptive refinement of both mass and force resolution.

Variants of the multiresolution approach include moving-mesh algorithms (Gnedin 1995, Pen 1995, Gnedin & Bertschinger 1996) in which the mesh used for computing the potential and force is allowed to deform. By contracting in regions of high particle density, the mesh can sample the gravitational field with higher resolution. Xu (1997) solved the Poisson equation on an unstructured mesh. In these codes, the irregularity of the mesh leads to force errors that are difficult to control, but their adaptivity and high dynamic range make these methods interesting for further study and development.

2.1.5 OTHER GRAVITY SOLVERS Various other methods have been proposed and used for computing gravitational forces. Several methods are based on multipole expansions (see Sellwood 1987), but those methods that pick out a preferred center are generally inappropriate for cosmology. The fast multipole method of Greengard & Rokhlin (1987) has attracted considerable attention, but the $O(N)$ scaling of the original algorithm erodes in the presence of strong clustering. Adaptive multipole methods appear promising but so far have seen no use in cosmology.

More exotic approaches include direct integration of the collisionless Boltzmann equation (Hozumi 1997), treatment of collisionless dark matter as a pressureless fluid (Peebles 1987b, Gouda 1994), and even treating gravitating matter as a quantum fluid obeying the Schrödinger equation (Widrow & Kaiser 1993, Davies & Widrow 1997). These methods are useful in providing insight to the physics of gravitational clustering but are not meant to compete with other techniques as a method of general simulation.

2.2 *Gas Dynamics*

The first cosmological simulations with gas dynamics were one-dimensional, plane-parallel treatments of gas and dark matter flows in the sheet-like caustics ("Zel'dovich pancakes") that form as the first nonlinear structures in models with purely large-scale initial density fluctuations (e.g. Doroshkevich et al 1978). Shapiro et al (1983) and Bond et al (1984) modeled the combined growth of baryon-neutrino pancakes in a universe dominated by massive neutrinos, showing that only a small fraction of the baryons would be able to cool

in the postshock regions of these pancakes. In one dimension, even these early simulations were able to include detailed treatments of ionization, recombination, radiative and Compton cooling, and thermal conductivity (Shapiro & Struck-Marcell 1985).

The strong nonlinearity of the gas dynamical equations, manifested in the ubiquity of oblique shock waves in cosmological simulations, makes it difficult or impossible to develop numerical methods whose accuracy and convergence can be proven. Computational gas dynamics is art more than science. For this reason, testing of algorithms against simple (one-dimensional) problems with exact solutions, as well as comparison of different codes against each other, is essential to proving their validity. A comparison of several cosmological gas dynamics codes was performed by Kang et al (1994); a more extensive project is underway currently by Frenk et al (CS Frenk, SDM White, P Bode, JR Bond, GL Bryan, et al, unpublished manuscript).

In comoving coordinates, the cosmological fluid equations are

$$\frac{\partial}{\partial t}\left(\frac{\rho_b}{\bar{\rho}_b}\right) + \frac{1}{a}\vec{\nabla}\cdot\vec{v}_b = 0,$$

$$\frac{\partial \vec{v}_b}{\partial t} + \frac{1}{a}\vec{v}_b\cdot\vec{\nabla}\vec{v}_b + H\vec{v}_b = -\frac{1}{a\rho_b}\vec{\nabla}p + \vec{g}, \tag{3}$$

where ρ_b, $\bar{\rho}_b$, $\vec{v}_b$, and p are the (baryonic) mass density, mean mass density, peculiar velocity, and pressure, respectively, and $\vec{g}$ is the gravitational field (Equation 1). These must be supplemented by either an energy or entropy equation. Outside of shocks, these take the form

$$\frac{\partial u}{\partial t} + \frac{1}{a}\vec{v}_b\cdot\vec{\nabla}u = -\frac{p}{a\rho_b}\vec{\nabla}\cdot\vec{v}_b + \frac{1}{\rho_b}(\Gamma-\Lambda),$$

$$\frac{\partial S}{\partial t} + \frac{1}{a}\vec{v}_b\cdot\vec{\nabla}S = \frac{1}{p}(\Gamma-\Lambda). \tag{4}$$

For a perfect gas with ratio of specific heats γ, the thermal energy and entropy per unit mass are $u = p/[(\gamma-1)\rho_b]$ and $S = (\gamma-1)^{-1}\ln(p\rho_b^{-\gamma})$, respectively. Artificial viscosity is often added to Equation 4 to generate the entropy needed across shock waves. In nonadiabatic calculations, heating and cooling rates per unit volume Γ and Λ and all they depend on, such as ionization and chemistry rate equations, radiative transfer, etc, must be included.

2.2.1 SMOOTH-PARTICLE HYDRODYNAMICS Smooth-particle hydrodynamics (SPH) is a Lagrangian (particle-tracking) method for integrating the fluid equations invented by Lucy (1977) and Gingold & Monaghan (1977). The fluid variables (baryon density, velocity, temperature, etc) are followed using particles of fixed mass representing fluid elements. The method is therefore an

extension of *N*-body methods, making it relatively easy to add SPH to existing cosmological simulation codes. SPH has been reviewed by Monaghan (1992).

The first cosmological SPH codes were written by Evrard (1988), who combined gas dynamics with a P^3M code, and by Hernquist & Katz (1989), who based their SPH on a tree code (see also Katz et al 1996a). Since then, many other groups have added SPH to cosmological simulation codes (Thomas & Couchman 1992, Steinmetz & Müller 1993, Couchman et al 1995, Serna et al 1996, Shapiro et al 1996, Steinmetz 1996, Tissera et al 1997). Recently, several parallel implementations have been developed (Pearce & Couchman 1997, Davé et al 1997a, Nakasato et al 1997).

Because SPH is Lagrangian, the mass continuity equation (the first of Equation 3) is obviated. The baryonic mass density is estimated by treating each particle as spread out with a smoothing kernel *W*:

$$\rho_b(\vec{x}\,) = \sum_{i=1}^{N} m_i W\left(\vec{x} - \vec{x}_i, h\right), \tag{5}$$

where m_i and $\vec{x}_i$ are, respectively, the particle mass and position, and h is a smoothing length. A kernel of compact support such as a spline is used so that the sum extends only over particles closer than some cutoff radius proportional to h. These particles are easily found from neighbor lists constructed with the tree or P^3M algorithms. The smoothing length generally is taken to vary with $\rho_b^{-1/3}$ so that a fixed number of particles (typically 30–40) is included in the kernel sum. Numerical issues associated with variable smoothing length have been discussed by many authors, including Hernquist (1993), Steinmetz & Müller (1993), and Serna et al (1996). A stability analysis has been performed by Balsara (1995), who provided suggestions for optimal parameters. The resolution of SPH has been improved significantly by Shapiro et al (1996) by using an adaptive ellipsoidal rather than spherical smoothing kernel and by switching off artificial viscosity for all particles except those that are in or about to enter shocks. Navarro & Steinmetz (1997) have also found improvements after reducing the amount of artificial shear viscosity.

The accuracy of SPH is more difficult to assess than for Eulerian (fixed-grid) hydrodynamics algorithms because of the absence of any rigorous proof of convergence to the solutions of the fluid equations in the continuum limit. Comparisons with other algorithms (e.g. Kang et al 1994) suggest that while SPH allows for very high-density contrasts, it suffers from poor resolution of shocks as well as low resolution in low-density regions. Nonetheless, its relative ease of implementation, combined with its high resolution in dense regions, makes SPH an excellent practical method for cosmological gas dynamics.

2.2.2 EULERIAN GRID ALGORITHMS Finite-difference methods have long been used to provide numerical approximations of the Eulerian fluid equations for computational fluid dynamics (Richtmeyer & Morton 1967). Cosmological gas flows are often highly supersonic; the gas falling into clusters of galaxies is shock-heated from 10^4 to 10^8 K. Robust schemes are needed to ensure the correct treatment of shocks and other discontinuities (e.g. contact discontinuities, across which the density and temperature jump but not the pressure, and tangential discontinuities, across which the tangential velocity changes). A variety of reliable methods have been developed and tested extensively in the computational fluid dynamics community (e.g. Sod 1985, LeVeque 1992).

The first multidimensional applications of these methods to cosmology, using artificial viscosity for the treatment of shocks, were made by Ryu et al (1990), Cen et al (1990), and Yuan et al (1991). Ryu et al used the multidimensional flux-corrected transport method (Sod 1985). Cen et al used an approach developed in aeronautical engineering by Jameson (1989) and detailed by Cen (1992). Yuan et al used ZEUS-2D, a radiation-magnetohydrodynamics code developed by Stone & Norman (1992), with modifications described by Anninos & Norman (1994). All of these early cosmological gas dynamics codes were robust and performed reasonably well on simple tests. However, they did not resolve shocks as well as modern shock-capturing methods based on solution of the Riemann problem for the evolution of fluid discontinuities (Landau & Lifshitz 1959) without explicit artificial viscosity (e.g. LeVeque 1992). Hence efforts have shifted to the implementation of newer algorithms.

Two approaches have been used for high-resolution shock-capturing algorithms in cosmology: total-variation diminishing (TVD) schemes and the piecewise parabolic method (PPM). In both schemes, the gas dynamical equations are written in conservation law form, i.e. $\partial u^i/\partial t + (\partial/\partial x^j)F^{ij}(u) = 0$, where u^i is a vector of densities (mass, momentum, and energy) and F^{ij} is a vector of fluxes for these densities. Fluxes are computed across cell boundaries to update the cell-average densities. Terms such as cosmological expansion, heating and cooling, and gravity may be included as source terms using the method of operator splitting with fractional timesteps (Richtmeyer & Morton 1967).

In TVD schemes, the fluxes are computed using an approximate solution of the Riemann problem, with corrections added to ensure that there are no postshock oscillations. The TVD codes of Ryu et al (1993) and Quilis et al (1994, 1996) are "second-order" accurate away from shocks, meaning that as the mesh spacing is reduced by a factor f, the numerical truncation errors go down by a factor f^2. More importantly, perhaps, they resolve shock jumps correctly in just two grid zones.

The PPM algorithm (Collela & Woodward 1984, Woodward & Collela 1984) is a third-order accurate extension of the Godunov method (LeVeque 1992).

The Riemann problem at cell boundaries is solved accurately using a quadratic interpolation of the cell-average densities that is constrained to minimize (but not entirely eliminate, unlike TVD) postshock oscillations. Away from shocks, PPM is third-order accurate. Shocks are resolved slightly better than in lower-order TVD codes. PPM has been implemented in cosmology by Bryan et al (1995) and Sornborger et al (1997).

2.2.3 ADAPTIVE GRID ALGORITHMS Eulerian methods give the most accurate solution of the gas dynamical equations for a given resolution, but they suffer from the resolution limit of the grid. Current simulations generally use at most 512^3 grid cells (with a few heroic runs of larger size on parallel machines), whereas cosmologists need a spatial dynamic range of 10^4 or more to follow galaxy formation. Two variations of grid-based hydrodynamics have been employed to increase the resolution: mesh refinement and deformable moving meshes.

Mesh refinement is discussed above in the context of solving the Poisson equation (Sections 2.1.3 and 2.1.4). Such methods have been used for more than a decade in computational fluid dynamics. Their first application to cosmological gas dynamics was made by Anninos et al (1994), who used a two-level hierarchy of cubic grids for solving the fluid equations with higher resolution in an interesting simulation subvolume. The subvolume was taken to be fixed in space and present throughout the simulation, and a three-dimensional implementation of the ZEUS code with second-order accurate fluxes was used for the gas dynamics solver. Their method was a first step toward fully adaptive mesh refinement in which refinement grids are placed (and removed) dynamically at multiple levels of refinement where needed during the course of a simulation. With PPM as the gas solver, adaptive mesh refinement has recently been demonstrated by Bryan & Norman (GL Bryan & ML Norman, unpublished manuscript, astro-ph/9710187). They achieved a peak dynamic range of 8192^3 using grids of size 64^3 or less. Their method is very promising for future high-resolution studies of cosmological gas dynamics.

An alternative approach to higher resolution is to allow the mesh to deform with the flow. Gnedin (1995) has developed a moving mesh hydrodynamics solver in which the grid locally expands and contracts so as to approximately track the flow of gas without the grid crossing itself. Such methods may offer the advantages of both SPH (high resolution owing to its Lagrangian nature) and Eulerian codes (shock capturing in two grid zones), although severe mesh distortion leads to new errors that need further study.

2.2.4 OTHER GAS DYNAMICS ALGORITHMS Several other algorithms have been used for approximate or phenomenological treatments of cosmological gas

dynamics. One early approach was the method of "sticky particles" in N-body codes, whereby particles labeled as gaseous are allowed to collide inelastically when sufficiently close. Based on the local density and temperature estimated from the pair separation and relative velocity, the colliding pair may be merged together (Blumenthal et al 1986). Alternatively, the relative kinetic energy may be dissipated and the gas particles converted into "stars" (i.e. made collisionless) at sufficiently high density (Carlberg 1988a,b, Carlberg & Couchman 1989). A more sophisticated approach is the "beam scheme" in which the gas is represented by sampling the microscopic Maxwellian velocity distribution at several discrete values in each cell of the simulation volume. Mass, momentum, and energy are transported according to kinetic theory (Sanders & Prendergast 1974). This method has been applied in cosmological simulations by Vishniac et al (1985) and Chiang et al (1989); compared with Eulerian finite-difference methods, it has relatively large numerical viscosity. A still more sophisticated method, based on gas kinetic theory applied on an unstructured mesh, has been used by Xu (1997). In one-dimensional simulations, Xu's method resolves shocks in about two mesh cells.

2.3 *Additional Physics*

Besides gravity and adiabatic gas dynamics, atomic and radiative processes are very important in the formation of galaxies and the evolution of the intergalactic medium. In particular, radiative cooling is thought to be primarily responsible for the condensation and survival of galaxies within larger virialized structures (e.g. White & Rees 1978, Blumenthal et al 1984). The processes included in state-of-the-art cosmological simulation codes include optically thin radiative cooling, multispecies chemistry, a phenomenological treatment of star formation and its associated energy feedback, and approximate radiative transfer.

The simplest way to incorporate radiative cooling is by means of an equilibrium cooling function $\Lambda(T)$ such that the cooling rate per unit volume is $n_e n_p \Lambda(T)$, plus a contribution proportional to $n_e(T - T_\gamma)$ from Compton cooling of ionized gas by the microwave background radiation. In this approach, the number densities of free electrons and protons, n_e and n_p, respectively, are computed assuming equilibrium between recombination and collisional ionization at temperature T (with T_γ the microwave background temperature), which eliminates the need to follow rate equations for multiple species. Cooling functions were used in many early dissipative simulations, e.g. by Cen et al (1990) and Katz & Gunn (1991), and continue to be adequate for many applications.

The cooling function approach breaks down when ionization equilibrium breaks down, as can happen behind shocks or in dense cooling regions, and when photoionization becomes more important than collisional ionization, as it does in the tenuous intergalactic medium. Gnedin (1996a) accounted for the second

effect by generalizing the cooling function to depend on the photoionization rate while retaining a one-fluid treatment of the gas. However, a full treatment of cooling requires following the nonequilibrium abundances of free electrons and all atomic, ionic, and molecular species relevant for cooling. Cen (1992) was the first to implement such a treatment in a cosmological simulation code, including rate equations for electrons and all ionization states of hydrogen and helium. Haehnelt et al (1996b) added heavier elements ("metals"), with their photoionization equilibria computed using the code CLOUDY (Ferland et al 1998).

Because of the importance of molecular hydrogen as a coolant of primordial (i.e. metal-free) gas below 10^4 K (e.g. Peebles & Dicke 1968, Shapiro & Kang 1987), recent treatments add H^-, H_2^+, and H_2 (Haiman et al 1996, Abel et al 1997, Anninos et al 1997, Gnedin & Ostriker 1997). All species are treated as though they are in the ground electronic state (although recombination rates are computed including cascades from excited states), which is a good approximation at the low densities of cosmological and intergalactic gas (Abel et al 1997).

Gas heating can also be important, both in raising the Jeans mass enough to suppress dwarf galaxy formation (e.g. Couchman & Rees 1986, Dekel & Silk 1986, Kepner et al 1997a) and in reionizing the intergalactic medium (Shapiro & Giroux 1987, Ostriker & Gnedin 1996). Heating by star formation (ultraviolet radiation from hot stars, stellar wind bubbles, and supernovae) has been included in a phenomenological way, along with the conversion of gas into collisionless particles representing stars or galaxies, by many workers, e.g. Katz (1992), Cen & Ostriker (1992a, 1993b), Navarro & White (1993), and Mihos & Hernquist (1994).

Radiative transfer has been treated so far only in relatively crude approximations because the specific intensity is computationally infeasible, as it is a function of six variables (position, photon frequency, and direction) and time. Cen (1992) treated the radiation field as spatially homogeneous and isotropic while allowing for its detailed energy dependence, an approximation that has been used frequently since. Gnedin & Ostriker (1997) treated radiative emission as uniform and isotropic but allowed absorption to vary locally depending on the gas density, using a clever scheme they call the local optical depth approximation.

In one (Ducloux et al 1992) or two (Stone et al 1992) space dimensions, improved treatments of radiative transfer have been developed using a variable Eddington factor (the ratio of radiation stress to energy density). In these codes, the Eddington factor, needed to close the radiation moment hierarchy at second order, is provided by approximate integrations of the radiative transfer equation that are valid in both the optically thick and thin regimes. So far this very promising method has not included the full frequency dependence of the

radiation, nor has it been extended to three dimensions, which both require substantial increases in computation.

2.4 *Initial Conditions*

Initial conditions for simulations of structure formation consist of specifying the background cosmological model and the perturbations imposed on this background. The background model is generally taken to be a spatially flat or open Robertson-Walker spacetime with specified composition of dark matter, baryons, a possible cosmological constant, etc. Specifying such a model requires more than just the two numbers H_0 and Ω (or the deceleration parameter q_0); at the very least the amount and nature of dark matter must be given (Trimble 1987).

At very high redshift, e.g. at $z \approx 1100$ when recombination has occurred and photons decouple from baryons, small-amplitude ("linear") density fluctuations were present in each component (baryons, photons, massless neutrinos, dark matter). The statistical nature of these fluctuations depends, of course, on how they were generated. Two classes of early universe models are widely considered to provide plausible mechanisms: inflation (Guth 1981) and topological defects (Vilenkin & Shellard 1994). Inflation predicts Gaussian fluctuations, while defect models are non-Gaussian.

Gaussian fluctuations are simple, as they are specified fully by one function, the power spectrum $P(k)$. In Gaussian models, the fluctuations are set down ab initio (perhaps 10^{-35} s after the Big Bang) and evolve straightforwardly thereafter. In real space, the joint probability distribution of density fluctuations at N points is a multidimensional Gaussian (i.e. multivariate normal distribution). Because the covariance matrix of this Gaussian becomes diagonal in Fourier space, it is very easy to sample a Gaussian random field by sampling its Fourier components on a Cartesian lattice (Peacock & Heavens 1985, Bardeen et al 1986). Salmon (1996) has implemented an alternative method based on convolving a white noise process, with the advantage that it can work for arbitrary spatial sampling. Pen (1997) has implemented Salmon's method with FFT convolution, truncating the convolution window in such a way as to improve the sampling of long-wavelength waves in periodic boxes.

Non-Gaussian models are much more complicated. Not only do they require more information than the power spectrum, physical models also require costly computation. For example, topological defects induce matter density fluctuations from the time of their creation in the early universe all the way to the present day. The dynamics of defect formation and evolution are relativistic and fully nonlinear, requiring large-scale simulations to compute. Two classes of defect models have received the most attention: cosmic strings and global textures. The dynamic range requirements for cosmic string simulations

starting before recombination and proceeding to low redshift are daunting (Allen & Shellard 1990, Bennett & Bouchet 1990). As a result, models for string initial conditions have been studied relatively little (e.g. Albrecht & Stebbins 1992a,b). Global textures are somewhat easier to simulate and have been included in cosmological structure formation simulations by Park et al (1991), Cen et al (1991), and Gooding et al (1992).

Weinberg & Cole (1992) proposed a simple phenomenological class of non-Gaussian models: local nonlinear transformations of Gaussian random fields. In these models, unlike topological defects, the fluctuations are seeded in the early universe. They are easy to compute and provide useful comparisons against Gaussian models in order to assess effects of non-Gaussianity in simple control models.

Once the linear density fluctuation field has been specified at some initial time (at $z \sim 100$ for typical high-resolution simulations), dark matter particle positions and velocities must be obtained along with baryon density, velocity, and temperature fields. The standard approach for the dark matter is to displace equal-mass particles from a uniform Cartesian lattice using the Zel'dovich (1970) approximation (Doroshkevich et al 1980, Dekel 1982, Efstathiou et al 1985):

$$\vec{x} = \vec{q} + D(t)\vec{\psi}(\vec{q}), \qquad \vec{v} = a\frac{dD}{dt}\vec{\psi} = aHfD\vec{\psi}, \tag{6}$$

where $\vec{q}$ labels the unperturbed lattice position, $D(t)$ is the growth factor of the linear growing mode, and $f = d\ln D/d\ln a \approx \Omega^{0.6}$ is its logarithmic growth rate (Peebles 1980). The irrotational (curl-free) displacement field $\vec{\psi}$ is computed by solving the linearized continuity equation,

$$\vec{\nabla}\cdot\vec{\psi} = -\frac{\delta}{D(t)}, \tag{7}$$

where $\delta(\vec{x},t) = [\rho(\vec{x},t) - \bar{\rho}]/\bar{\rho}$ is the relative density fluctuation. The displacement field is readily evaluated from Equation 7 using Fourier transform methods. The baryon velocity field is computed in a similar way, and the baryon temperature is generally initialized to the (redshift-dependent) microwave background temperature or to about 10^4 K if the gas is ionized.

An alternative treatment of the dark matter sets the initial displacements to zero but gives the particles variable masses in proportion to $(1+\delta)$. The velocity for the linear growing mode is then proportional to the gravity field, $\vec{v} = -(Hf/4\pi G\bar{\rho})\vec{g}$. This method has been used by Warren et al (1992), who showed that it led to statistically indistinguishable results from the particle displacement method.

When particles are distributed initially on a lattice, the small-scale periodicity of the lattice persists visibly until virialization occurs, i.e. until particles fall

into and orbit in gravitationally bound objects. To avoid this artificial pattern, particles may be perturbed from a random Poisson distribution instead of a lattice. However, the Poisson noise itself is a seed for gravitational instability, adding unwanted power to the desired spectrum. This noise may be eliminated by arranging the particles initially, before applying displacements, in a random "glass" state with very small gravitational forces. A gravitational glass is made by advancing particles from random positions using the opposite sign of gravity until they "freeze" in comoving coordinates (Baugh et al 1995, White 1996).

For some purposes, constraints may be imposed on the initial fluctuation field, e.g. that the simulation volume contain a rare high density peak on a scale $\sim 10\ h^{-1}$ Mpc that will form a cluster of galaxies. Many independent realizations could be generated until one arises that closely satisfies the desired constraint by chance. An equivalent procedure is to use the method of constrained random fields. Bertschinger (1987) introduced an iterative but inefficient algorithm for constrained Gaussian random fields. Binney & Quinn (1991) showed that the sampling of peaks simplifies considerably when spherical coordinates are used, allowing a faster algorithm. A real breakthrough was made by Hoffman & Ribak (1991), who devised a relatively simple exact algorithm for sampling Gaussian random fields with arbitrary linear constraints [Salmon (1996) independently discovered the same trick]. The Hoffman-Ribak algorithm has been implemented in publicly available codes by van de Weygaert & Bertschinger (1996). Ganon & Hoffman (1993) have extended the algorithm to the case of many (hundreds or more) constraints specified on a regular lattice, in order to provide initial conditions for simulations matching the large-scale density or velocity fields of our own Universe. Sheth (1995) has extended the Hoffman-Ribak algorithm to local nonlinear transformations of Gaussian random fields.

The last ingredient that needs specification for most models is the matter power spectrum *P(k)*, which is related (but not equal) to the mean squared amplitude of the Fourier transform of density fluctuations (Bertschinger 1992):

$$\langle \delta(\vec{k})\delta^*(\vec{k}')\rangle = P(k)\delta_D(\vec{k}-\vec{k}'), \tag{8}$$

where δ_D is the Dirac delta function and angle brackets denote an ensemble average. [Each realization of $\delta(\vec{x})$ or $\delta(\vec{k})$, including the one that describes our own Universe at early times, is a random sample of an ensemble.] A factor of $(2\pi)^3$ may be included with $P(k)$ in Equation 8 if an alternate Fourier transform convention is used. With the definition of Equation 8, the variance of density measured with a window function $W(kR)$, when, for example, averaging over a sphere of radius R (equation 21.52 of Peebles 1993), is

$$\sigma^2(R) = \int d^3k\, P(k) W^2(kR). \tag{9}$$

In much (though not all) of the cosmology literature, d^3k (Equation 9) is divided by $(2\pi)^3$, and $P(k)$ is defined as larger by the same factor.

In Gaussian models, the post-recombination density field is the linear convolution of the primordial fluctuation field with a transfer function. (Slightly different transfer functions apply for CDM and baryons because of the finite Jeans length for baryons.) The power spectrum used to initialize simulations therefore generally takes the form

$$P(k, t_i) = Ak^n |T(k, t_i)|^2 . \tag{10}$$

The primordial spectral slope $n = 1$ leads to curvature fluctuations of constant amplitude on all scales (Harrison 1970, Zel'dovich 1972). Because inflation occurred for only a finite duration, simple models predict a value slightly less than $n = 1$, and power-law inflation or other variants can readily produce "tilts" with $0.7 < n < 1.2$ (Steinhardt 1995). The transfer function is normalized so that $T(0) = 1$. For CDM models, $k^2T(k)$ approaches a constant on small scales (e.g. Bardeen et al 1986).

The amplitude A of the primordial power spectrum is not specified by inflation or other models. Conventionally, it has been fixed one of two ways. The first is to require that the relative density fluctuations at redshift zero, averaged over a sphere of radius 8 h^{-1} Mpc and computed using linear perturbation theory (i.e. using the simple linear transfer function T of Equation 10 with t_i set equal to the present time), equal the inverse of the "linear bias factor" b (defined and discussed below): $\sigma_8 = 1/b$. The motivation for this choice is the observations that galaxy counts show fluctuations of unit amplitude in 8 h^{-1} Mpc spheres (Davis & Peebles 1983) and the matter fluctuations are smaller by a factor b in the linear bias model. A more direct physical normalization has been possible since the measurement of microwave background anisotropy by the *Cosmic Background Explorer* (*COBE*) (Smoot et al 1992, Bunn & White 1997).

Transfer functions have been published by many workers; a useful early compendium was provided by Holtzman (1989). Such tables and fitting formulae have been superceded by publicly available codes that compute matter transfer functions and microwave background anisotropy (COSMICS by Ma & Bertschinger 1995, CMBFAST by Seljak & Zaldarriaga 1996). On a cautionary note, models with HDM (massive neutrinos) require more than just the transfer function; the HDM particles must be given a thermal distribution of momenta. For an accurate treatment, this distribution should itself be perturbed by gravitational effects (Ma & Bertschinger 1994a; see also Ma 1996).

Many papers have been written assessing structure formation models based on linear perturbation theory, the Press-Schechter theory (Press & Schechter 1974), and so on. Recent reviews of variants of CDM have been written by Liddle et al (1996a–c).

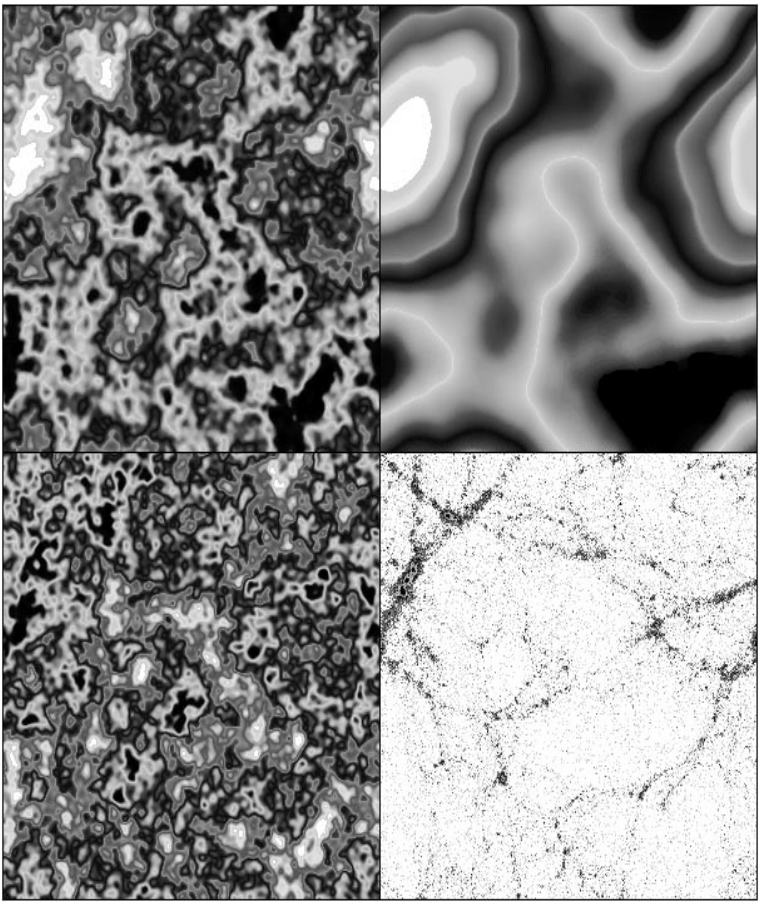

Figure 2 Evolution of the potential and density in a simulation of a hot plus cold dark matter (HCDM) universe in a cube 50 h^{-1} Mpc across. *Top left*: scale-invariant gravitational potential fluctuations in the early universe. *Top right*: Post-recombination potential, showing the modulation by the transfer function. *Bottom left*: Post-recombination density fluctuations. *Bottom right*: Nonlinear density field at redshift 0, from a simulation with $\Omega_\nu = 0.2$ by Ma & Bertschinger (1994b).

The roles of gravity, the transfer function, and linear and nonlinear evolution may be seen in Figure 2, which shows how the primordial scale-invariant fluctuations are modulated in several stages, to produce finally a tapestry of filaments, clusters, and voids.

2.5 *Numerical and Physical Limitations*

Cosmological simulations suffer from limited dynamic range, numerical errors, and neglected physics. These effects have recently begun to receive greater

attention as increasing computer power enables more rigorous testing. The introduction of gas dynamics into simulation codes has also presented a new set of numerical issues, stimulating practitioners to assess more carefully the limitations of their results.

In purely gravitational *N*-body simulations of structure formation, the numerical issues include dynamic range, force accuracy, and time integration accuracy. Most codes use the leapfrog scheme (Section 2.1); although this is much less accurate than the high-order schemes used for globular cluster or Solar System integration, tests suggest that with a timestep small enough so that all particles travel less than a softening length each timestep, the statistical results of cosmological interest converge (Quinn et al 1997). Most workers tune their force evaluation algorithm to have pairwise errors of at most a few percent (e.g. Pearce & Couchman 1997), which Hernquist et al (1993) concluded is adequate given the masking effect of two-body relaxation. This leaves dynamic range as the biggest concern. Three distinct kinds of dynamic range are needed for a faithful simulation: mass resolution (number of particles), initial power spectrum sampling (range of wavenumbers present in the initial conditions), and spatial resolution (force-softening length compared with box size).

Mass resolution was perhaps the most severe problem when simulations had fewer than 10^5 equal-mass particles, but it is giving way to the relentless advance of technology ($N = 10^9$ will become the standard on supercomputers within a very few years) and to multimass methods (e.g. Katz et al 1994, Splinter 1996). Particle masses of $10^9\ M_\odot$ or less are probably satisfactory for simulating the gross dynamics of halos of galaxies like the Milky Way, and this resolution is readily available today.

Resolution of the initial power spectrum is related to the mass resolution because the initial density field is sampled at the particle positions. Little et al (1991) suggested that initial high-frequency power is unimportant on scales that become nonlinear, although Splinter et al (1998) argued to the contrary. Tormen & Bertschinger (1996) and Cole (1997) suggested ways to extend the sampling of the initial power spectrum by adding long waves to an evolved simulation.

Force resolution is probably the most significant dynamic range issue for *N*-body simulations [although Melott & Shandarin (1989) argued that mass resolution is equally important]. Resolving the dynamics of galaxies in simulations sufficiently large to sample large-scale tidal fields requires 1-kpc resolution in boxes of size 100 Mpc, a dynamic range of 10^5 in length scale, about a factor of 10 beyond the current state of the art of high-resolution codes. Smaller force softening requires more timesteps (Quinn et al 1997) and leads to increased two-body relaxation (Huang et al 1993). The practical figure of merit is the ratio of force softening distance to mean interparticle spacing. With P^3M and tree codes, this ratio is typically set to about 0.1, while with PM codes, it is about unity. Most practitioners have accepted the benefits of higher-resolution

enabling codes to follow gravitational collapse to high density. Low force resolution leads to excessive merging of halos (e.g. Carlberg 1994, Gelb & Bertschinger 1994a, Zurek et al 1994, Moore et al 1996). However, Melott et al (1997) showed that high resolution leads to spurious heating and fragmentation for the collapse of planar Zel'dovich pancakes, and they advocated a force softening no smaller than the mean interparticle spacing. Splinter et al (1998) found less dramatic effects with realistic three-dimensional initial conditions, yet they also concluded that cosmological *N*-body simulations cannot be trusted on scales smaller than the mean interparticle spacing. While not all would agree, the issues they raise merit further investigation.

When gas dynamics is added, several new types of errors can arise. The most obvious (and also often the most subtle) are numerical problems with the hydrodynamics algorithm, which can best be diagnosed by testing against exact solutions and other codes (Kang et al 1994; CS Frenk, SDM White, P Bode, JR Bond, GL Bryan, et al, unpublished manuscript). Two-body relaxation of dark matter can also cause spurious heating of the gas solely by the gravitational coupling; Steinmetz & White (1997) studied this effect and advised on the resolution requirements to avoid it.

Self-gravity and cooling lead to potential problems for gas dynamics codes. Gnedin & Bertschinger (1996) demonstrated the need for consistent treatment of gravity and hydrodynamics in order to ensure local energy conservation. Bate & Burkert (1997) compared SPH with an Eulerian code and showed that SPH may give incorrect results unless the minimum resolvable SPH mass is less than the Jeans mass. Truelove et al (1997) found a similar requirement for Eulerian hydrodynamics by using adaptive mesh refinement, as did Owen & Villumsen (1997) in two-dimensional simulations using SPH for gas coupled with PM for dark matter. Evrard et al (1994) had previously noted the strong resolution dependence of gas dynamical results for cold self-gravitating gas. Even in a cluster in hydrostatic equilibrium, Anninos & Norman (1996) found that the X-ray luminosity depends strongly on numerical resolution. Clearly these resolution effects need further study.

With gravity and cooling but no heating or star formation, the baryons in high-resolution simulations collapse to high density, impeding further progress (e.g. Katz & White 1993). Recent work has focused on the role of photoionization heating in suppressing galaxy formation (Efstathiou 1992; Navarro & Steinmetz 1997 and references therein). In the course of investigating these effects, Weinberg et al (1997a) discovered an interplay between mass resolution, photoionization, and radiative cooling that led to incorrect results on galaxy formation when photoionization was included at low resolution. Their experience is a cautionary reminder that when physics is added or codes are run in a new regime, careful testing must precede astrophysical conclusions.

2.6 *Biased Galaxy Formation*

Biased galaxy formation refers to phenomenological models of galaxy formation in simulations (or analytic theories) that lack sufficient resolution or physical content to allow galaxies to form directly. Crudely speaking, "bias" as used in this context refers to the difference between the galaxy distribution and that of all matter. Although the current trend is toward more realistic modeling of galaxy formation, biasing models are still used in large-box *N*-body simulations, analytic theories, and analysis of redshift survey data. For these reasons, we include a brief discussion to conclude this section on numerical simulation algorithms.

Bias was originally invoked to explain the stronger correlations of galaxy clusters compared with galaxies themselves. Kaiser (1984) showed that the regions of high density (plausibly those regions that preferentially form galaxies) in a Gaussian random field are more strongly correlated than the overall field itself. Dekel & Rees (1987) reviewed the motivation and physical mechanisms for biased galaxy formation. In recent years, bias has been used most commonly in the context of the linear bias model, where, on scales larger than a few megaparsecs, the galaxy density fluctuations are enhanced over those of the mass by a factor b, the linear bias factor:

$$\frac{\delta n_g}{\overline{n}_g} = b\left(\frac{\delta\rho}{\rho}\right). \tag{11}$$

Local nonlinear biasing models were investigated by Coles (1993). Mo & White (1996) and Kauffmann et al (1997) devised an analytic model of bias based on the Press-Schechter formalism.

Bardeen et al (1986) proposed that galaxy formation occurs at the peaks of the initial density field smoothed on a galactic mass scale. This "peak bias" model has been used in *N*-body simulations to tag a fraction of particles as galaxies (Davis et al 1985, Park 1991, Suginohara & Suto 1991). White et al (1987a) found that bias arose naturally when enough resolution was present to identify dense dark matter halos forming within the simulations. However, Katz et al (1993) showed that the association between dense halos and initial peak particles is poor. Moreover, beginning with Carlberg & Couchman (1989), many groups have found that the halos formed in dark matter simulations are actually antibiased with respect to the mass, i.e. $b < 1$, because of excessive merging of halos compared with real galaxies. They also showed that the root-mean-square (rms) velocities of dark matter halos may be substantially less than those of the mass, a phenomenon called cosmological velocity bias (Couchman & Carlberg 1992, Summers et al 1995).

While biased galaxy formation remains a useful phenomenological model, recent emphasis has shifted toward cosmological simulations with gas and cooling

where dense baryonic clumps plausibly representing galaxies form without need for a biasing model. Indeed such simulations permit the measurement of the biasing factor (or scale-dependent bias function) itself (e.g. Cen & Ostriker 1992a, Tissera et al 1994, Summers et al 1995, Gnedin 1996b). Although numerical simulation of galaxy formation will always rely on phenomenological treatments of star formation and stellar energy feedback processes, these are considerably more direct and physical than current biased galaxy formation models and may one day obviate the need for biasing schemes.

3. ANALYSIS TECHNIQUES

Cosmic structure formation models are stochastic: The initial conditions are random (albeit with well-specified statistical properties), and their evolution is chaotic. No realistic model would claim to predict the exact structures we see in our Universe; at best, theorists can hope to construct models of the Universe that "look like" the real thing. But how is this vague test quantified? Many statistics have been devised for this purpose. In this section, a brief summary of methods is presented; a more complete review was given by Coles (1992).

Table 1 lists the major statistics applied in cosmological simulations of structure formation. They are distinguished by whether they are most naturally applied to continuous fields such as the density fluctuation field $\delta(\vec{x})$ or to a set of discrete points (e.g. galaxies or simulation particles). In practice these applications are interchangeable because a point set can be convolved with a window function to produce a continuous field, and a continuous field may be Poisson sampled (with spatially-varying Poisson density) to produce a point set (e.g. Bertschinger 1992). Other statistics apply exclusively to the internal properties of galaxies, clusters, or dark matter halos. Some statistical measures associated with specific physical measurements (e.g. the column density distribution of Lyα absorption lines or the distribution of gravitational lens separations) are discussed in Section 5.

3.1 *Statistics Using Particle Positions*

The spatial properties of a statistically homogeneous set of points (galaxies or simulation particles) is fully characterized by the N-point correlation functions (Peebles 1980). The best known of these is the two-point correlation function, which is measured to be well fit by a power-law $\xi(r) = (r/r_0)^{-\gamma}$ with $\gamma = 1.8$ and $r_0 \approx 5\,h^{-1}$ Mpc (Totsuji & Kihara 1969; Peebles 1980 and references therein). This statistic has been widely used in cosmic structure formation simulations beginning with those of Miyoshi & Kihara (1975). The standard method to compute ξ is based on counting pairs as a function of pair separation, with subsampling if the total number of pairs is prohibitively large; Ruffa &

Table 1 Statistical measures applied to galaxies and numerical simulations of structure formation

Category	Statistic	Name	Reference
Particle positions	$\xi(r)$	Two-point correlation function	Peebles 1980
	$P(k)$	Power spectrum	Bertschinger 1992
	$\zeta(r_1, r_2, r_3)$	Three-point correlation function	Groth & Peebles 1977
	$B(k_1, k_2, k_3)$	Bispectrum	Peebles 1980
	ξ_N, $\bar{\xi}_N$	N-point correlation functions and moments	Peebles 1980
	$P_0(V)$, $P_N(V)$	Void probability function, cell counts	White 1979
	—	Percolation, minimal spanning tree statistics	Coles 1992
	—	Multifractal statistics	Martínez et al 1990
Density fields	$G(\nu)$	Genus of isodensity surfaces	Melott 1990
	—	Area of isodensity surfaces	Ryden 1988
	$v_i(\nu)$	Minkowski functionals	Mecke et al 1994
	$f(\delta)$	One-point density distribution	Kofman et al 1994
	$\left\langle \delta_c^N \right\rangle$	One-point cumulants (skewness, kurtosis, etc)	Peebles 1980
	—	Shape statistics	Davé et al 1997b
Velocity fields	$f(v)$	One-point velocity distribution (and moments)	Inagaki et al 1992
	$\mathcal{M}$	Mach number	Ostriker & Suto 1990
	$f(\theta)$	Velocity divergence distribution (and moments)	Bernardeau et al 1985
	$f(v_{12})$, σ_{12}	Pairwise radial velocity distribution and dispersion	Davis & Peebles 1983
Redshift space	$\xi(r_p, \pi)$, $\xi(s)$	Redshift space correlation functions	Davis & Peebles 1983
	$P_s(k, \mu)$	Redshift space power spectrum	Cole et al 1995
Clusters or halos	$n(m)$	Mass distribution	Press & Schechter 1974
	$n(V_c)$	Circular velocity distribution	Gelb & Bertschinger 1994a
	$n(\sigma)$	Velocity dispersion distribution	Evrard 1989
	$n(T)$, $n(L)$	Temperature and X-ray luminosity distributions	Cen & Ostriker 1994a

Porter (1993) devised a fast algorithm based on a tree code. Simulations not only use the correlation function as a comparative statistic, they also can test the reliability of estimators of ξ applied to observational samples (e.g. Mo et al 1992). The three-point correlation function can be measured in simulations by counting triplets (e.g. Efstathiou & Eastwood 1981), but higher-order correlations are more efficiently estimated and characterized by their volume averages, the irreducible moments (cumulants) of counts in cells $\bar{\xi}_N$ (Peebles 1980).

The power spectrum and two-point correlation function are Fourier transform pairs. From this fact, the incorrect conclusion may be reached that they are interchangeable in practice. Estimates of the two-point correlation function require subtracting off the number of pairs for a Poisson distribution. This requires knowing the mean density accurately when the correlation amplitude is low, i.e. on large scales. Large-scale sample variations ("cosmic variance") make it difficult to estimate this density in any finite-size survey (but see Hamilton 1993 for an estimator that is relatively insensitive to this effect). The correlation function is most accurately measured in the strong-clustering regime, $\xi > 1$. The power spectrum estimate involves no such subtraction of unclustered pairs; therefore it offers a reliable estimate of clustering to the longest wavelengths probed by a survey, subject to the caveat of cosmic variance (i.e. sampling fluctuations) and to practical details of sample geometry. The power spectrum is widely used as a measure of structure in numerical simulations as well as for comparison with observations (e.g. Gramann & Einasto 1992, Vogeley et al 1992, Baugh & Efstathiou 1994). The Fourier transform of the three-point correlation function is known as the bispectrum (e.g. Fry et al 1993).

The distribution of counts in cells, $P_N(V)$, gives the probability of finding N objects in a randomly placed volume V of fixed shape. This set of statistics provides an alternative and very useful characterization of clustering. Interest in this cell count distribution grew after a simple prediction of its form was made by Saslaw & Hamilton (1984), based on a thermodynamic theory of gravitational clustering (see Sheth & Saslaw 1996 for a refinement of the theory). Although the thermodynamic theory has been met with skepticism, it has spurred the development of many alternative hierarchical scaling theories as well as their investigation in cosmological simulations (e.g. Itoh et al 1988, Suto et al 1990, Bouchet & Hernquist 1992, Ueda et al 1993, Bromley 1994, Colombi et al 1995, Ueda & Yokoyama 1996).

The void probability function $P_0(V)$ contains information about all $\bar{\xi}_N$ and is fully determined by them when these moments exist (White 1979). (Here "void" should not be thought of in the sense of the large underdense regions of the galaxy distribution. Instead it refers to any volume that contains no objects—galaxies or simulation particles—whatsoever. Observationally, of course, a luminosity limit must be stated to make this statement meaningful.) The void

probability function has been studied extensively in numerical simulations combined with analytical models of hierarchical clustering (e.g. Bouchet et al 1991, Einasto et al 1991, Weinberg & Cole 1992, Colombi et al 1996a).

Additional statistics of point processes are provided by percolation analysis (Zel'dovich et al 1982) and related statistics based on the minimal spanning tree (Pearson & Coles 1995, Bhavsar & Splinter 1996; Krzewina & Saslaw 1996 and references therein). These approaches "connect the dots" with short line segments. There has been considerable discussion about the utility of percolation as a cosmological test, with some authors (e.g. Bhavsar & Barrow 1983, Dekel & West 1985) emphasizing difficulties and expressing doubts about its discriminating power, while others maintain its value (Dominik & Shandarin 1992, Yess & Shandarin 1996). Recently Sahni et al (1997) have proposed an extension of percolation, the volume fraction of the largest cluster or void defined at a given density threshold, that addresses some of the practical problems of the percolation length and relates percolation to topology.

The hierarchical scaling of correlation functions has inspired comparisons with statistical fractals (Peebles 1980 and references therein). The galaxy distribution cannot be a simple fractal because strong clustering on small scales gives way to homogeneity on large scales; the distribution is not scale invariant. However, over a limited range of scales it may be a multifractal, a clustered distribution having different scaling properties as a function of density (e.g. Jones et al 1988, Martínez et al 1990). Analytical theories and simulations (e.g. Bouchet et al 1991) suggest that there are two scalings, one for voids and one for clusters, described by the Hausdorff and correlation dimensions, respectively. Colombi et al (1992) gave an excellent summary of the numerical, statistical, and dynamical issues involved in testing whether the matter distribution in simulations (and, by extension, the Universe) is a bifractal.

3.2 *Statistics of Density Fields*

Turning next to statistics for continuous density fields, we note first that *N*-point correlation functions and power spectra are naturally defined and very useful in this case much as they are for point sets. A family of new statistics, reviewed by Melott (1990), is based on the two-dimensional surfaces of constant density (isodensity surfaces). The best known of these is the genus per unit volume $g(\nu)$ as a function of the standardized density contour level $\nu = \delta/\sigma$ (Gott et al 1986). The total genus G of a surface is a topological invariant measuring the number of "holes" (as in a doughnut) minus the number of isolated regions. One of its attractions is the fact that an exact prediction exists for the shape of $G(\nu)$ for Gaussian random fields (Doroshkevich 1970, Bardeen et al 1986, Hamilton et al 1986), enabling a test of Gaussianity on large scales where the matter distribution is expected to still approximate the linearly growing initial

conditions. When the smoothing scale is varied, the amplitude of the genus curve varies in a spectrum-dependent way, providing another useful clustering statistic. Computer programs for computing the genus are given by Melott (1990); an alternative and simpler algorithm is provided by Coles et al (1996).

Recent work has shown that the genus statistic is relatively insensitive to redshift-space distortions (Matsubara 1996), is slightly dependent on biasing (the relation of galaxies to mass, discussed below) (Park & Gott 1991), and is more sensitive to non-Gaussianity arising from nonlinear evolution of Gaussian initial conditions (e.g. Sahni et al 1997, Seto et al 1997) or from non-Gaussian initial conditions (Beaky et al 1992, Weinberg & Cole 1992, Matsubara & Yokoyama 1996, Avelino 1997). The area of isodensity contours provides an independent and useful statistic (Ryden 1988, Ryden et al 1989).

Minkowski functionals (Mecke et al 1994) have recently been introduced in cosmology as a very powerful descriptor of the topology of isodensity surfaces. In three dimensions, there are four Minkowski functionals (v_0, v_1, v_2, v_3); two of them are the genus (actually, its relative the Euler characteristic) and surface area statistics discussed above, and the other two are the covered volume (related to the void probability function) and integral mean curvature. Analytical results for Gaussian random fields have been provided by Schmalzing & Buchert (1997), who also have made available a computer program for computing these statistics from a point process. The insight and unification provided by these recent results suggests a promising future for Minkowski functionals as a statistic for both cosmological simulations and redshift surveys.

Perhaps the simplest (though incomplete) test of Gaussianity is simply to examine the one-point distribution function $f(\delta)d\delta$. When the density is defined by smoothing as a function of scale, one has the continuous analog of the counts in cell distribution $P_N(V)$. It has long been known that on scales of a few megaparsecs or less, $f(\delta)$ is strongly skewed toward positive values and is fit well by a lognormal distribution such that $\log(1+\delta)$ has a normal (Gaussian) distribution. Coles & Jones (1991) discussed the properties of lognormal random fields. While lognormal primordial fluctuations can be envisaged (Weinberg & Cole 1992), simulations show that nonlinear evolution of Gaussian initial conditions produces a $f(\delta)$ that is intriguingly well fitted by the lognormal form (Kofman et al 1994, Ueda & Yokoyama 1996). Bernardeau & Kofman (1995) have shown from perturbation theory and the Zel'dovich approximation that this agreement is fortuitous.

Low-order moments of $f(\delta)$, particularly the skewness (the third moment), have also been studied extensively (e.g. Coles & Frenk 1991, Coles et al 1993, Juszkiewicz et al 1993, Luo & Vishniac 1995; see Lokas et al 1995 for the irreducible fourth moment, the kurtosis). With these, Juszkiewicz et al (1995) obtained good approximations to the mildly nonlinear $f(\delta)$ by using a series

expansion. Protogeros & Scherrer (1997) considered a class of local Lagrangian approximations in which the nonlinear density of a mass element is a function only of its initial density contrast and time. By choosing this function so that low-order moments agree well with perturbation theory, they obtained a model for $f(\delta)$ that agrees well with simulations in the mildly nonlinear regime (Protogeros et al 1997).

Visual inspection of galaxy redshift surveys and projected catalogs gives a clear impression of filamentary and sheet-like structure. Consequently, several statistics have been developed that aim to quantify such structure. Recent work has been summarized by Davé et al (1997b), who explored moment-based shape statistics devised by several groups, as well as their own new filament statistics. These statistics degrade under sparse sampling but are promising discriminators of models, particularly with the large redshift surveys expected to become available within a few years.

3.3 *Velocity Statistics*

The spatial statistics listed above make use of only half the phase space coordinates of particles, neglecting velocity information (or, in redshift space, using radial velocity in place of distance). Although it is difficult to measure sufficiently accurate extragalactic distances to obtain reliable peculiar velocities (Strauss & Willick 1995), different cosmological models vary substantially in their predictions (especially as a function of the density parameter Ω), making investigation of peculiar velocities well worthwhile.

The simplest velocity statistic is the velocity distribution of single particles, $f(v)4\pi v^2 dv$ where v is the magnitude of peculiar velocity. This statistic is poorly studied despite the fact that it is the lowest-order distribution function appearing in the BBGKY kinetic theory of gravitational clustering (Peebles 1980). Either the radial component or one Cartesian component may be used instead of the magnitude of the three-dimensional velocity; because of isotropy, all three distributions are simply related. Inagaki et al (1992) and Raychaudhury & Saslaw (1996) compared the predictions of the thermodynamic theory of Saslaw & Hamilton (1984) with simulations starting from Poisson initial conditions, and they found good agreement. Cen & Ostriker (1993c) examined $f(v)$ for galaxies formed in their CDM simulations and noted that an exponential distribution fits better than a Maxwellian.

Davis et al (1997) have proposed using the small-scale velocity dispersion σ_1, the second moment of $f(v)$ after filtering out long-wavelength velocity contributions, to provide an estimate of Ω through the Layzer-Irvine cosmic energy equation. In practice, they measure this single-particle dispersion using a single-particle weighting of a pairwise velocity. This statistic has the advantage of being less sensitive to sampling fluctuations from clusters of galaxies than the

pair-weighted pairwise velocity dispersion (e.g. Zurek et al 1994, Somerville et al 1997). Alternatively, a redshift dispersion may be measured as a function of density, as suggested by Kepner et al (1997b).

Besides examining the velocities of individual particles or galaxies, study is possible of the "fluid" or "bulk flow" velocity obtained by averaging the velocity over a window of radius R, $\vec{V}(R)$. Kofman et al (1994) showed analytically and with N-body simulations that in the mildly nonlinear regime, the distribution of $\vec{V}$ remains close to Maxwellian for Gaussian initial conditions. The steep decline of the Maxwellian for bulk flows that are much larger than the rms leads to a sensitive test of power on large scales (e.g. White et al 1987b, Bertschinger & Juszkiewicz 1988). Other velocity field statistics include the cosmic Mach number $\mathcal{M} = V(R)/\sigma(R)$, where $\sigma(R)$ is the small-scale velocity dispersion within the same window (Ostriker & Suto 1990). Bulk flows are sensitive to large-scale power, while small-scale dispersions are sensitive to smaller scales, so $\mathcal{M}$ is sensitive to the shape of the power spectrum.

Another statistic applied to the large-scale velocity field is the distribution of velocity divergence, $f(\theta)d\theta$ where $\theta = \vec{\nabla} \cdot \vec{v}$ (Bernardeau 1994). The velocity divergence is attractive theoretically because in the linear regime, it is proportional to the density fluctuation (see Equations 6 and 7); in the mildly nonlinear regime for Gaussian initial conditions, the ratio of its skewness to the square of its variance is sensitive to Ω (Bernardeau et al 1995, 1997); and for a potential flow (as expected on large scales for gravitationally induced motions), the velocity field is fully described by $\theta(\vec{x})$ (Bertschinger & Dekel 1989).

The statistics of relative velocities of pairs of galaxies have been extensively studied on small scales because of the possibility of measuring Ω using the cosmic virial theorem (Peebles 1980), which relates these velocities to the two- and three-point correlation functions. The relative velocity of a pair separated by $\vec{r}$, $\vec{v}_1 - \vec{v}_2$, is decomposed into a component along $\vec{r}$ and the remainder perpendicular to it. The distribution of $v_{12} \equiv \hat{r} \cdot (\vec{v}_1 - \vec{v}_2)$, in particular its mean $\langle v_{12} \rangle$ and standard deviation σ_{12}, has been studied extensively in numerical simulations, initially by Davis et al (1985) and more recently by others, including Zurek et al (1994), Gelb & Bertschinger (1994b), Brainerd et al (1996), and Colin et al (1997). The sensitivity of σ_{12} to rich clusters makes it difficult to measure well but also provides discriminating power among different structure formation models (Somerville et al 1997). Sheth (1996) recently has provided analytical insight into the exponential form of $f(v_{12})$ by using an extension of the Press-Schechter theory (Press & Schechter 1974; cf also Mo et al 1996).

3.4 *Redshift Space Distortions*

A few words may be said here about both the challenges and opportunities afforded by the "redshift space distortions" arising when redshift is used in

place of distance. The effects of peculiar velocities on the two-point correlation function have been extensively studied with simulations (e.g. Suto & Suginohara 1991, Bahcall et al 1993, Matsubara 1994). To characterize these effects, it is useful to distinguish redshift differences along the line of sight (π) and perpendicular to it (r_p), leading to the two-dimensional correlation function $\xi(r_p, \pi)$ (Davis & Peebles 1983). The effects of peculiar velocities on the power spectrum were first investigated analytically by Kaiser (1987), who showed that the anisotropy of $P_s(k, \mu)$ (where $\cos^{-1}\mu$ is the angle between $\vec{k}$ and the line of sight) in the quasilinear regime (i.e. on large scales) depends simply on $\beta \equiv f(\Omega)/b \approx \Omega^{0.6}/b$, where b is the linear bias parameter. This effect has been studied thoroughly in simulations (e.g. Bahcall et al 1993, Cole et al 1995, Brainerd et al 1996). The measured spectrum contains information about both the spatial clustering and β; both are important to obtain from redshift surveys. Gramann et al (1994) have explored means of undoing the redshift space distortion on large scales to recover the real-space density. Cole et al (1994) focused instead on practical determination of β.

3.5 *Internal Properties of Galaxies, Halos, or Clusters*

The next set of statistics listed in Table 1 refers to the internal properties of galaxies or galaxy clusters. In cosmological simulations, galaxies must be identified according to some prescription in order to apply these statistics. Thus the first question is how to identify dense objects in simulations. When baryons are present with high resolution and cooling, this problem is greatly simplified (at the expense of a much costlier simulation) by the condensation of cold gas in dark matter potential wells.

In simulations with only dark matter, several algorithms have been proposed for identifying objects, including the friends-of-friends linking algorithm used by Davis et al (1985), extensions devised by Barnes & Efstathiou (1987), methods based on spherical overdensity (e.g. Warren et al 1992, Lacey & Cole 1994), and the DENMAX algorithm of Bertschinger & Gelb (1991) (and modified by Governato et al 1997, who have publicly released their code called SKID). The reader must exercise caution in "galaxy" or "halo" results from simulations without baryons because of the strong merging of dark matter halos and the dependence of this process on resolution and method of halo identification (e.g. Gelb & Bertschinger 1994a, Summers et al 1995).

Given a set of galaxies or clusters, all the particle statistics listed in Table 1 may be applied and compared with those applied to other classes of objects (e.g. galaxies versus mass) in order to deduce the relative bias. This issue is discussed further in Section 2.6. However, the distribution functions can also be measured for internal properties of the composite objects including mass (e.g. Press & Schechter 1974, Brainerd & Villumsen 1992) or, for clusters,

the number of members (the multiplicity function of Bhavsar et al 1981 is a logarithmic number distribution). For objects with "isothermal" density profiles $\rho \propto r^{-2}$, the total mass is divergent, but the circular speed $V_c = (GM/r)^{1/2}$ is constant and provides an alternative to mass (Frenk et al 1988, Gelb & Bertschinger 1994a, Ueda et al 1994). For clusters of galaxies, the velocity dispersion, temperature, and luminosity provide alternative statistics whose distributions provide tests of theory against observations (Evrard 1989, Peebles et al 1989, Cen & Ostriker 1994a).

4. TESTING OF COSMOLOGICAL MODELS

During the 1980s the dominant use of cosmological simulations was to test models of structure formation, particularly the CDM model. While simulations have proven to be much more versatile in recent years, model testing remains an important application.

Perhaps the first test of a cosmogonical model should be whether it is sufficiently well posed to enable meaningful simulation in the first place. Phenomenological models must be formulated precisely within a consistent physical framework (e.g. explosive galaxy formation models). Sometimes the fundamental physics is known but is too complex to allow for fully satisfactory simulation, given the limitations of current computers and numerical algorithms (e.g. superconducting cosmic strings). It is possible that even the best current simulations vastly oversimplify the physics needed for reliable structure formation models. However, the detailed comparison of these models with data suggests that such a view is overly pessimistic. Recent high-resolution simulations compare remarkably well with many aspects of the observed galaxy distribution.

4.1 *Cold Dark Matter*

The CDM model became the platform on which simulations of cosmic structure formation matured into a powerful theoretical tool during the 1980s. It is not reviewed extensively here, as accounts have been given already by Frenk (1991), Davis et al (1992a), Liddle & Lyth (1993), and Ostriker (1993). However, a brief discussion of the CDM model and its shortcomings is worthwhile to motivate study of the currently popular alternatives.

The CDM model adopts parameter values $H_0 \approx 50$ km s^{-1} Mpc^{-1} and $\Omega_c = 1 - \Omega_b \approx 0.95$, where Ω_c and Ω_b give the present mean mass density of CDM and baryons, respectively, normalized to the critical density $8\pi G/3H_0^2$. Prior to the *COBE* measurement of temperature anisotropy (Smoot et al 1992), the only significant free parameter in the CDM model was the normalization of the power spectrum, conventionally specified by the rms relative mass density fluctuation

in a sphere of radius $R_8 = 8\,h^{-1}$ Mpc, $\sigma_8 = \sigma(R_8)$, computed using Equation 9 with the power spectrum extrapolated to the present day assuming linear theory. When set to the observed value based on galaxy counts, $\sigma_8 = 1$, the CDM model predicts excessive peculiar velocities for galaxies (Davis et al 1985). A similar conclusion follows from the cosmic virial theorem, which implies $\Omega \approx 0.3$ if galaxies are a fair tracer of the clustering and dynamics of the mass (Peebles 1986). However, Carlberg et al (1990) and Couchman & Carlberg (1992) found in their high-resolution simulations that dark matter halos have substantially smaller velocities than the mass, an effect they termed velocity bias. During this same period, evidence accumulated that the $b = 1/\sigma_8 = 2.5$ "standard biased" CDM model favored by Davis et al (1985) lacked sufficient power on large ($\sim 50\ h^{-1}$ Mpc) scales to explain the observed clustering (Maddox et al 1990, Saunders et al 1991) or velocity fields (Lynden-Bell et al 1988) of galaxies.

Without exotic physics such as gravitational radiation produced in "tilted" inflationary models, the large–angular-scale microwave background anisotropy measurements pinned down the normalization of CDM models to $\sigma_8 \approx 1.2$ (Wright et al 1992, Bunn & White 1997). With a strong velocity bias, interest revived in "unbiased" ($b \approx 1$) CDM models. Several groups explored the constraints imposed by small-scale clustering, pairwise velocities, the circular velocity and mass distributions of galaxies, galaxy cluster masses, etc (e.g. Bahcall & Cen 1993, Cen & Ostriker 1993c, Brainerd & Villumsen 1994a,b, Gelb & Bertschinger 1994a,b, Zurek et al 1994). From this and additional work, the consensus has emerged that the unbiased CDM model is ruled out because it has too much power on small scales.

4.2 *Variants of Cold Dark Matter*

Based on the *COBE* results combined with smaller-scale constraints from galaxies, galaxy clusters, and large-scale structure, it has become apparent that there are several ways to modify the CDM model to reduce its excessive small-scale power (Efstathiou et al 1992, Wright et al 1992). These include "tilting" the primordial power spectrum index to $n < 1$ (TCDM), replacing some of the CDM with HDM that clusters much less efficiently on small scales (HCDM), replacing some of the CDM with a cosmological constant Λ that does not cluster at all (LCDM), and simply eliminating most of the matter, leaving an open universe (OCDM). All these models retain the assumption of "adiabatic" primeval perturbations of the sort produced during inflation (Guth & Pi 1985). Dodelson et al (1996) have recently reviewed the status of the expanded family of CDM models.

The most obvious way to reduce small-scale power, while retaining consistency with the large-scale power required for microwave background anisotropy,

is to decrease the primeval spectral index n of Equation 10, which is a possibility allowed by inflationary models. The TCDM model has been investigated with simulations by Cen et al (1992), Cen & Ostriker (1993a), Gelb et al (1993), and Moscardini et al (1995). Based on their results and the more recent summaries by White et al (1995) and Cole et al (1997), it appears that TCDM models with $0.7 \leq n \leq 0.9$ remain viable, although they are less attractive than some of the other alternatives.

The HCDM model is attractive because the extra ingredient added to the CDM model is a particle that is known to exist and whose abundance is predicted in standard cosmology, the neutrino. The twist is that one or more flavors of neutrino must have nonzero masses adding up to $18.7\,h^2(\Omega_\nu/0.2)$ eV, where Ω_ν is the fraction of the critical mass density in massive neutrinos. The first simulations of this model, performed by Davis et al (1992b), Jing et al (1993), and Klypin et al (1993), showed that with $\Omega_\nu = 0.3$, the HCDM model is in better agreement with observations of pairwise velocities and large-scale structure than the CDM model. Bryan et al (1994) showed that this model also succeeds in reproducing the observed abundance of X-ray clusters. However, simulations by Cen & Ostriker (1994b), Ma & Bertschinger (1994b), and Klypin et al (1995) showed that galaxy formation occurs too late unless Ω_ν is decreased in order to increase the small-scale power. HCDM with $\Omega_\nu = 0.2$ (with one or two massive neutrino flavors) remains an attractive model, although it may overproduce rich clusters (Cen & Ostriker 1994b, Borgani et al 1997). Liddle et al (1996b) gave a recent review.

Although an astrophysically interesting cosmological constant $\Lambda \neq 0$ is very unnatural in particle physics, cosmologists are attracted by its ability to increase the age and size of the Universe for a fixed H_0 as well as providing for a spatially flat model ($\Omega_b + \Omega_c + \Omega_\Lambda = 1$ with $\Omega_\Lambda = \Lambda/3H_0^2$) with low matter density (Efstathiou et al 1990, Carroll et al 1992, Ostriker & Steinhardt 1995). First simulated by Davis et al (1985), this model has attracted a great deal of attention in the 1990s (e.g. Martel 1991, Suginohara & Suto 1992b, Cen et al 1993a, Cen & Ostriker 1994a, Gnedin 1996a,b). The preferred value of Ω_Λ is around 0.6–0.7, although its optimal range is still a subject of debate (e.g. Klypin et al 1996, Liddle et al 1996c).

The OCDM model with $\Omega = \Omega_b + \Omega_c \approx 0.2$ is attractive in that it requires no ingredients beyond the baryons observed and inferred from primordial nucleosynthesis and the dark matter inferred in clusters of galaxies. The case for an open universe has been presented in a review by Coles & Ellis (1994); simulations have been performed by Davis et al (1985), Martel (1991), Bahcall & Cen (1992), Kauffmann & White (1992), and Cole et al (1997). Although the simplest versions of inflation favor $\Omega = 1$ (Guth 1981), recent interest has developed among theorists in open-universe inflationary models compatible

with microwave background constraints and structure formation (Liddle et al 1996a).

4.3 *Other Models*

Currently less popular structure formation models include several Gaussian and non-Gaussian models. The oldest one is the hot dark matter (HDM) model, with all the dark matter in the form of massive neutrinos with a free-streaming length (the collisionless analog of the Jeans length) of several megaparsecs. The HDM model was the first physically motivated model studied with simulations (Melott 1982, White et al 1983, 1984). Recent work supports the early conclusion that galaxy formation occurs too late because of the absence of initial small-scale power (e.g. Cen & Ostriker 1992b).

If CDM has too much small-scale power and HDM too little, perhaps a Goldilocks solution exists with warm dark matter. Colombi et al (1996b) investigated warm models with a range of free-streaming lengths (hence varying degrees of suppression of small-scale power). They found that models tuned to match large-scale structure have too much power on small scales.

Peebles (1987a) proposed a low-density model without nonbaryonic dark matter, with $\Omega_b \approx 0.1$ and primeval "isocurvature" fluctuations corresponding to a spatially varying entropy per baryon. Structure formation simulations of this isocurvature baryon model by Suginohara & Suto (1992a) and Cen et al (1993b) indicated some difficulties, but the greatest conflict arises with the microwave background (Hu et al 1995).

Several classes of non-Gaussian models have been explored. Early simulations of structure formation with cosmic strings assumed that loops acted as accretion sites (e.g. Scherrer et al 1989), but later work showed that long strings are dominant (e.g. Albrecht & Stebbins 1992a,b). Cosmic textures, another type of hypothetical topological defect, also act as seeds (e.g. Gooding et al 1992), and generic seed models have been explored by Villumsen et al (1991). Recently, Cen (1997b) has shown that models with random seeds cannot account for the strong clustering of rich galaxy clusters.

Other non-Gaussian models include local nonlinear transformations of Gaussian random fields (e.g. Moscardini et al 1991, Weinberg & Cole 1992). While less physically motivated than the other models discussed above, they provide useful foils for assessing the effect of nonlinear gravitational evolution in producing non-Gaussianity from Gaussian initial conditions.

The discussion given above is only a partial summary of nonstandard structure formation models that have been considered. Nonetheless, a general conclusion applies: No model has emerged as a popular alternative to the generalized CDM models discussed in Section 4.2. Their initial conditions are more complicated, and when evolved, they show no compelling advantages to the variants of

CDM models. However, nature need not be so kind as to always favor the simplest theories we can conceive. For this reason, it remains valuable to explore nonstandard models with a close eye on observational signatures that can be tested.

5. APPLICATIONS

Cosmological simulations have numerous applications besides testing of structure formation models. This section presents some of the applications that have become active areas of research. Space limitations preclude discussing many other valuable and often ingenious uses of simulations.

5.1 *Clusters of Galaxies*

Rich clusters of galaxies are the most massive virialized objects in the Universe. At the same time, they are sufficiently young, and the relevant physics sufficiently simple (compared, for example, with galaxy formation), so that present-day simulations are effective in exploiting them as a probe of initial conditions. A great many papers have applied structure-formation simulations to clusters of galaxies because of their power to constrain cosmological parameters, including Ω, Ω_b, and σ_8 (the power spectrum normalization).

Numerical simulations of galaxy clusters have been used for the following goals, among others: (*a*) understanding the general processes of formation and evolution of single clusters (galaxy evolution and dynamics, intracluster medium); (*b*) testing observational methods of mass estimation (for both dark matter and baryons); (*c*) using the distribution of X-ray temperature (or luminosity, mass, or cluster velocity dispersion) and its evolution to constrain cosmological parameters; and (*d*) using substructure, morphology, shape, or radial profile to constrain cosmological parameters.

The first cosmological simulations of cluster formation with gas were performed by Evrard (1990) and Thomas & Couchman (1992), both of whom combined P^3M for gravity with SPH for gas dynamics. These and later simulations (Frenk et al 1996 and references therein) have explored several issues, including the equilibrium and distribution of the hot intracluster gas, the cluster response to mergers, and, in simulations with radiative cooling (Katz & White 1993, Frenk et al 1996), the survival of dissipatively condensed galaxies within dense cluster cores. Figure 3 shows maps of a simulated X-ray cluster at several epochs.

Observers and theorists have devoted much attention to the ratio of velocity dispersions of galaxies and gas, $\beta \equiv \sigma^2/(kT/\mu m_p)$, where σ is the one-dimensional velocity dispersion of galaxies in the cluster, T is the gas temperature, μ is the mean molecular weight, and m_p is the proton mass. (Note that

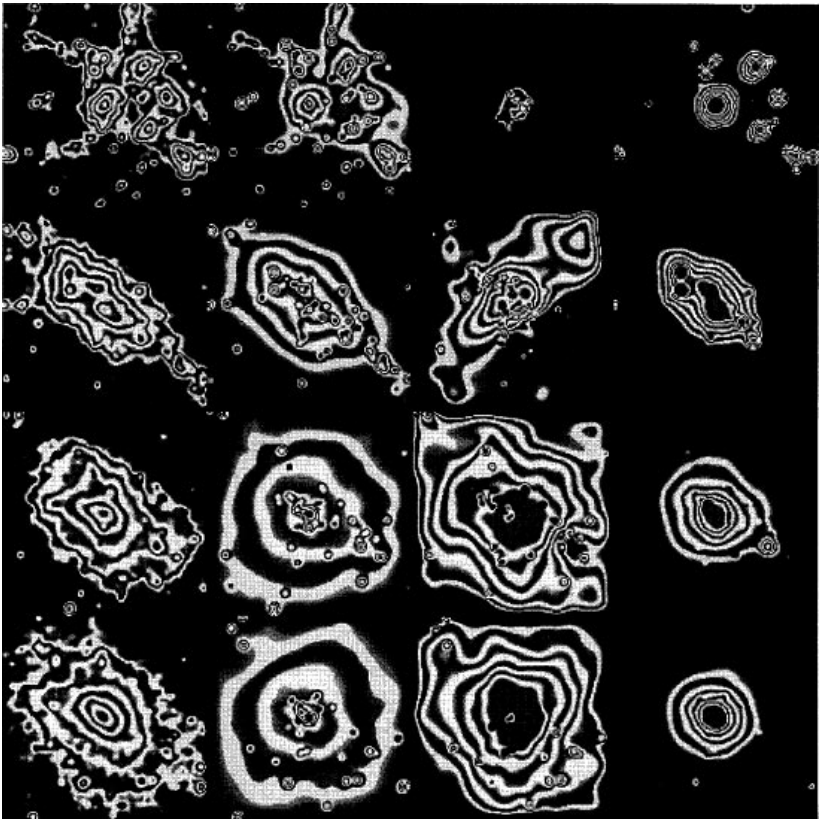

Figure 3 Evolution of an X-ray cluster in the standard cold dark matter (CDM) model. *Columns* from left to right show the projected dark matter density, projected baryon density, emission-weighted temperature, and predicted *ROSAT* X-ray surface brightness. *Rows* from top to bottom show the cluster at redshifts $z = 0.7$, 0.3, 0.1, and 0.03, respectively. From Frenk et al (1996).

this is a different use of the symbol β than in Section 3.4.) Direct measurement of this quantity in high-resolution simulations (e.g. Navarro et al 1995) yields $\beta \approx 1$, as expected for gas and galaxies that have fallen through the same potential. Values estimated from fitting the X-ray surface-brightness distribution yield underestimates by a variety of effects (Evrard 1990, Bahcall & Lubin 1994, Navarro et al 1995).

The reliability of cluster mass estimates based on X-ray observations of the hot gas when assuming hydrostatic equilibrium has been examined by several groups, including Tsai et al (1994), Evrard et al (1996), and Bartelmann &

Steinmetz (1996). Their papers show that the reliability of the deduced masses depends somewhat on how the X-ray surface-brightness profiles are fit but that accuracies of better than 25% are readily achievable. Bartelmann & Steinmetz (1996) and Cen (1997a) also argued that cluster projection effects systematically bias the ratio of masses estimated from X-ray data and gravitational lenses below unity (Bartelmann et al 1996 and references therein).

X-ray measurements of intracluster gas naturally provide an estimate of the gas density as well as the total binding mass. Including the relatively small contribution to baryons made by galaxies in luminous X-ray clusters, the baryon fraction of the mass is found to be

$$f_b = \frac{\Omega_b}{\Omega} \approx (0.06 \pm 0.003)\, h^{-3/2} \tag{12}$$

(White et al 1993b; Evrard 1997 and references therein). Simulations show that the baryon fraction in clusters is expected to vary little from the cosmic mean value (White et al 1993b, Cen & Ostriker 1994a). As White et al noted in the title of their paper ("The baryon content of galaxy clusters—a challenge to cosmological orthodoxy"), Equation 12 represents a challenge to cosmological orthodoxy, which favors $\Omega = 1$, $0.5 < h < 0.9$, and $\Omega_b \approx 0.015\, h^{-2}$ from standard Big Bang nucleosynthesis (Copi et al 1995). Although a recent measurement of the deuterium abundance in QSO absorption lines implies the higher value $\Omega_b \approx 0.019\, h^{-2}$ (Tytler et al 1996; S Burles & D Tytler, unpublished manuscript, astro-ph/9712109), even this value from Big Bang nucleosynthesis is incompatible with Equation 12 if $\Omega = 1$. However, the measured baryon fraction is perfectly compatible for an open universe or one with a cosmological constant, lending further support to the LCDM and OCDM models.

Rich clusters are rare objects corresponding to high-density peaks in the initial conditions. Their abundance is therefore highly sensitive to the normalization of the power spectrum. Because the virialized mass of rich clusters roughly equals the mass within a sphere of radius $8\, h^{-1}$ Mpc at the cosmic mean density, the cluster abundance and its evolution with redshift therefore provide a strong constraint on σ_8 (Evrard 1989, Bahcall & Cen 1992, White et al 1993a). The mean mass density parameter Ω enters the argument directly through the mass within the sphere; it enters indirectly through the scaling of fluctuations from the linear regime (implicit in σ_8) to the nonlinear regime of virialized clusters.

Conceptually, this cluster abundance test compares predicted and measured distributions of cluster masses (although X-ray luminosity or velocity dispersion may be used instead). Eke et al (1996) provided a comprehensive analysis leading to the conclusion

$$\sigma_8 = (0.52 \pm 0.04)\, \Omega^{-1/2}. \tag{13}$$

(Their exponent on Ω actually differs slightly from $-1/2$, and it depends weakly

on Ω and Λ.) Fan et al (1997) have shown recently that the rate of evolution of the cluster abundance depends on σ_8 but is insensitive to Ω, enabling the degeneracy between these parameters to be broken. They obtained $\sigma_8 = 0.83 \pm 0.15$ and $\Omega = 0.3 \pm 0.1$. These results are exciting, but a prudent observer may wish to wait for confirmation that we really know the cosmological parameters this well.

A different test of Ω was proposed by Richstone et al (1992), who noted that the presence of substructure in clusters argues that they are dynamically young. Because the growth of clustering slows greatly when $\Omega \ll 1$, if clusters indeed formed recently, this would favor a high Ω. This argument is qualitative, as there is neither a perfect measure of substructure nor a unique relation between substructure and age. Nevertheless, it has inspired much attention from simulators, beginning with Evrard et al (1993), who confirmed the qualitative connection between cluster morphology and Ω. Several groups have tested a range of statistical measures of substructure (with either galaxy counts or X-ray data) using simulations in an attempt to make a quantitative and robust test (e.g. Dutta 1995, Crone et al 1996, Buote & Tsai 1995, Pinkney et al 1996). The latest results appear to favor a low-density universe with $\Omega \approx 0.35$ (Buote & Xu 1997). In related work, Wilson et al (1996b) showed that reconstructions of cluster mass distributions by using weak gravitational lensing inversion should provide enough substructure information to allow a test of Ω.

5.2 *Gravitational Lensing*

Gravitational lensing provides a powerful way to study the distribution of matter in the Universe through the deflection of light from distant sources. There are many aspects of lensing, but only a few have been studied with cosmological simulations. An excellent (though already dated) review was given by Blandford & Narayan (1992). Here we summarize applications of simulations in two areas: strong gravitational lensing (formation of double images and long arcs) and weak lensing by clusters.

Cen et al (1994a) used cosmological simulations to estimate the frequency distribution of splitting angles for background QSOs lensed by the mass in their simulations. Their work extended an analytic treatment by Narayan & White (1988) based on the Press-Schechter formalism. Cen et al showed that, when the power spectrum is normalized by the *COBE* anisotropy, the CDM model predicts many lenses of separations greater than 8 arcsec, which contradicts observations. Wambsganss et al (1995) reached a similar conclusion based on simulated maps of the sky lensed by the mass distribution in their CDM simulation. Bartelmann et al (1995) used realistic cluster potentials from cosmological simulations to study the formation of arcs. They showed that the asymmetric cluster potentials greatly increase the frequency of arcs compared

with spherically symmetric models. Bartelmann & Steinmetz (1996) noted similarly that arcs form preferentially in clusters with substructure.

Kaiser & Squires (1993) developed a nonparametric method for reconstructing the projected mass distribution of clusters from the coherent weak distortions of background galaxies. Their work has inspired a large number of observational applications and theoretical tests and extensions. Bartelmann et al (1996) have proposed a reconstruction method for the projected mass distribution using chi-squared minimization of image stretching and magnification and tested it with simulations. Bartelmann (1995) used simulations to test the accuracy of cluster mass reconstructions, concluding that the Kaiser & Squires method and variants should provide accurate results. However, the smearing of images caused by atmospheric seeing causes a bias on the order of a factor of two that must be corrected (Wilson et al 1996a).

5.3 *Quasistellar Object Absorption Lines*

Our knowledge of QSO absorption line systems has increased tremendously in the last decade (see the review by Rauch 1998, in this volume). Structure formation simulations have played an important role in elucidating the nature of the Lyα forest of narrow hydrogen absorption lines, which are seen in spectra of QSOs at redshift $z > 2$. Early models of the forest were based on isolated spherical or sheet-like clouds. About a decade ago, hierarchical clustering models like CDM ones were realized to have small-scale structure that might readily produce clouds with abundance (Bond et al 1988) and clustering (Salmon & Hogan 1986) comparable to the Lyα forest lines. Another key was the realization by McGill (1990) that because of peculiar velocities, optically thin line profiles do not necessarily reflect the density profile of neutral hydrogen in space. Lines can form from velocity caustics (e.g. a structure that has just started to reverse the Hubble expansion) even if the gas is not particularly overdense.

Cosmological simulations of dark matter and gas with photoionization from the ultraviolet background (Cen et al 1994b, Zhang et al 1995, Hernquist et al 1996, Mücket et al 1996) have shown that the Lyα forest arises naturally from the filamentary web (Bond et al 1996) of structure that occurs in hierarchical clustering models with an appropriate amount of small-scale power. When the ratio of ionizing flux to baryon density is set near the observationally favored value, hierarchical models almost automatically predict the correct density distribution, redshift evolution, and clustering of the Lyα lines. Some of the lines form in well-defined clouds (particularly the damped lines; Katz et al 1996b), while others form in transient filamentary or sheet-like structures (Cen & Simcoe 1997), and still others are velocity caustics that may even be underdense in real space (Zhang et al 1995). Figure 4 shows

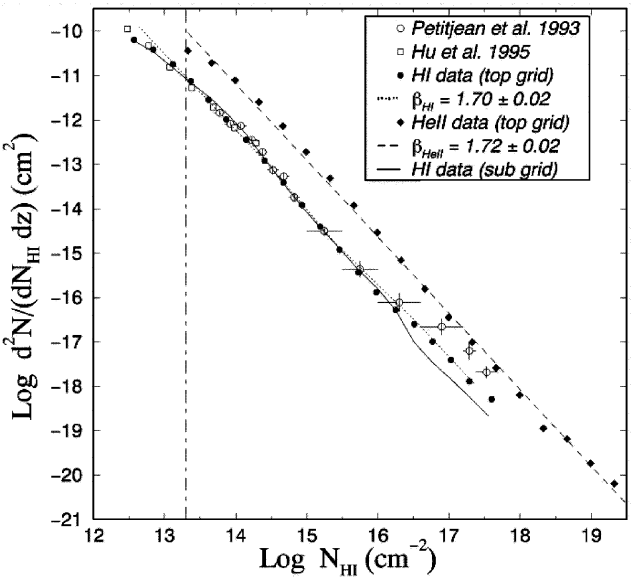

Figure 4 Simulated column density distribution of Lyα absorption lines (*filled circles* for H I, *diamonds* for He II) at redshift $z = 3$ in a standard CDM universe. Observational data are shown for H I (*open symbols*). From Zhang et al (1997).

the impressive match of simulated and measured column density distributions for the hydrogen Lyα line at $z = 3$, along with a prediction for ionized helium.

The success of numerical simulations has inspired analytical models that can account very well for the column density distribution and provide an understanding of how it arises (Bi et al 1995, Gnedin & Hui 1996, Bi & Davidsen 1997, Hui et al 1997). The agreement of analytical and numerical models with each other and with observational data is a remarkable success story that supports the hierarchical clustering models of structure formation. These results also show that the concept of a uniform medium producing continuous absorption, used by Gunn & Peterson (1965) to sharply limit the neutral hydrogen density in the intergalactic medium, must be replaced by absorption arising in a fluctuating medium (Reisenegger & Miralda-Escudé 1995, Rauch et al 1997b). There is, however, predicted to be a Gunn-Peterson trough for He II absorption (Miralda-Escudé et al 1996, Croft et al 1997, Zhang et al 1997). Requiring the Lyα forest to produce the observed overall opacity constrains the baryon abundance to $\Omega_b > 0.017\,h^{-2}$ (Rauch et al 1997b, Weinberg et al 1997b), which is consistent with the high value obtained by Tytler et al (1996).

The computational modeling has been extended to include the physics of metal lines with a sophisticated treatment of photoionization equilibrium (Haehnelt et al 1996a,b, Hellsten et al 1997, Rauch et al 1997a,b), Voigt-profile fitting to the simulated absorption-line spectra for rigorous comparison with observations (Davé et al 1997c), and the examination of correlations between close lines of sight (Charlton et al 1997).

The high column density-damped Lyα lines are thought to originate in dense gas associated with galaxies. Their abundance therefore can be used to constrain models of structure formation (e.g. Gardner et al 1997 and references therein).

5.4 *Radial Profiles of Dark Matter Halos*

Numerical simulations of hierarchical models (Section 4) show that most of the mass is drawn into dense clumps by gravity. The dark matter components of these clumps are identified with extended dark matter halos around galaxies (Frenk et al 1985). *N*-body simulations have allowed cosmologists to address a straightforward question: What is the shape of dark matter halos formed by hierarchical clustering? This question is relevant observationally to the cusps of elliptical galaxies (e.g. Faber et al 1997) and the profiles of clusters of galaxies.

Gunn & Gott (1972) and Fillmore & Goldreich (1984) presented analytical models for spherical "secondary" infall of collisionless matter onto a density peak in an expanding universe. Building on this work, Hoffman & Shaham (1985) proposed that virialized dark matter halos should have a power-law radial profile $\rho(r) \propto r^{-\nu}$, where ν is related to the logarithmic slope n of the power spectrum on the scales of interest. For $n < -1$, the slope relevant on galaxy scales in plausible models, the prediction of the secondary infall model is $\nu = 2$, corresponding to flat rotation curves such as those observed for the baryonic component of galaxies. For $n > -1$, the profiles steepen to $\nu = (9 + 3n)/(4 + n)$, corresponding to falling rotation curves.

The predictions of Hoffman & Shaham (1985) have been supported by many *N*-body simulations (e.g. Quinn et al 1986, Zurek et al 1988, Warren et al 1992, Crone et al 1994, Zaroubi et al 1996). However, high-resolution simulations (e.g. Frenk et al 1988) showed a steepening of the density profile with radius. Dubinski & Carlberg (1991) found that the halos formed in the CDM model have a logarithmic slope ν varying between 1 and 4, in good agreement with the Hernquist (1990) model. However, Navarro et al (1995, 1996) found instead a better fit to

$$\rho_{\rm NFW}(r) \propto \frac{1}{r(r + r_s)^2}, \tag{14}$$

where r_s is a scale radius. Their most surprising result was that this profile is universal for all hierarchical clustering models, regardless of the halo mass, the initial power spectrum, or cosmological parameters.

Navarro et al's results have been confirmed by Cole & Lacey (1996) and Kravtsov et al (1997) and in higher-resolution simulations by Tormen et al (1997) and Navarro et al (1997). The latter paper also shows that earlier work is, in fact, consistent with Equation 14. The characteristic density at $r = r_s$ correlates with mass in a way that reproduces the trends of the Hoffman & Shaham (1985) model. However, in a still higher-resolution simulation, Fukushige & Makino (1997) found that the profile remains steeper than r^{-1} to the limit of their resolution, and they attributed contrary results to two-body relaxation.

Why are the central profiles shallower than isothermal ($\nu = 2$)? Teyssier et al (1997) showed that when the Fillmore & Goldreich (1984) model is modified for gas, or dark matter with isotropic orbits, the limiting profile is $\nu = 1$ instead of $\nu = 2$. Alternatively, Evans & Collett (1997) examined the effect of diffusion driven by gravitational scattering and showed that the collisional Boltzmann equation of stellar dynamics has an attractor solution with $\nu = 4/3$.

Halo shapes and angular momenta have also been studied with *N*-body simulations (e.g. Barnes & Efstathiou 1987, Dubinski & Carlberg 1991, Warren et al 1992). Numerically simulated dark matter halos are found to be generally triaxial and slowly rotating.

5.5 *Self-Similar Clustering in Scale-Free Models*

Hierarchical clustering from scale-free initial conditions—initial power spectra $P(k) \propto k^n$ in an Einstein–de Sitter universe ($\Omega = 1$)—is expected to evolve in a self-similar way, with a unique length scale growing in comoving coordinates as $[a(t)]^\alpha$, $\alpha = 2/(3 + n)$ (e.g. Press & Schechter 1974, Efstathiou et al 1979, Peebles 1980, 1985). Although scale-free initial conditions differ from realistic models with a physical transfer function (Equation 10), they provide a theoretical laboratory for understanding nonlinear gravitational instability and have therefore been studied extensively.

One of the few analytical approaches to the strongly nonlinear regime is provided by self-similar solutions of the BBGKY hierarchy governing the growth of clustering (Peebles 1980). Making several approximations to close the hierarchy and render it tractable, Davis & Peebles (1977) obtained power-law solutions for the nonlinear correlation functions. Their key assumption was that on small scales, the mean proper velocity between pairs vanishes so that, on average, each particle has a fixed number of neighbors per unit volume. Under this assumption, known as stable clustering, the logarithmic slope of the nonlinear two-point correlation function is predicted to be $\gamma = (9 + 3n)/(5 + n)$. Higher-order correlation functions are expected to vary as $\xi_N \propto r^{-(N-1)\gamma}$, in agreement with the measured hierarchical scaling of correlation functions (Peebles 1980). The tempting conclusion is that the observed correlation function, with $\gamma = 1.8$, could be explained by stable clustering starting after recombination from white

noise ($n = 0$; Peebles 1974). However, *N*-body simulations show that scale-free initial conditions result in a varying slope of the nonlinear correlation function, approaching the predicted slope asymptotically only at very high values of ξ (Efstathiou & Eastwood 1981, Efstathiou et al 1988, Bertschinger & Gelb 1991).

The assumption of stable clustering has come under increased scrutiny recently. Padmanabhan et al (1996) concluded from their simulations that stable clustering is violated, while Jain (1997) concluded that it holds. Colombi et al (1996a) tested stable clustering and the predicted scaling of the *N*-point correlation functions as determined from the cumulants of counts in cells, and they found a departure from the predicted scaling but also showed that higher-resolution simulations are needed for a definitive test.

Stable clustering is one of the ingredients of a remarkable linear to nonlinear mapping of the correlation function introduced by Hamilton et al (1991). Guided by the simulation results of Efstathiou et al (1988), they showed how the initial linear correlation function may be deduced from the nonlinear evolved one and vice versa. Their method has been modified and tested with high-resolution *N*-body simulations by Jain et al (1995) and Padmanabhan (1996) and extended to the power spectrum and to universes with $\Omega < 1$ and $\Lambda \neq 0$ by Peacock & Dodds (1994, 1996). This body of work is important in enabling deduction of the initial power spectrum of fluctuations from the observed nonlinear spectrum (Peacock & Dodds 1994, 1996, Baugh & Gaztañaga 1996, Peacock 1997). However, its theoretical basis is not yet fully understood.

5.6 *Testing Approximations for Nonlinear Gravitational Dynamics*

Theoreticians devise approximations to nonlinear gravitational clustering with three purposes in mind: (*a*) to understand the nonlinear dynamics arising in simulations and thereby perhaps understand the Universe, (*b*) to replace expensive simulations with fast approximations, and (*c*) to relate the present-day distribution of galaxies directly to the initial conditions for structure formation. Many approaches have been adopted; only a brief and incomplete synopsis of recent work is given here. An early review was given by Shandarin & Zel'dovich (1989). Sahni & Coles (1995) provided an excellent comprehensive pedagogical review.

The Zel'dovich (1970) approximation (Equation 6) gives an accurate description of motion for pressureless dark matter (and even baryons or HDM on scales larger than the Jeans or free-streaming lengths). However, it breaks down once trajectories intersect; particles never turn around to orbit in bound systems. Several approximations have been suggested to cure this defect. The

first was to add an approximate viscosity term to the equation of motion to prevent trajectories from crossing (the adhesion approximation of Gurbatov et al 1989). A simpler method is to prefilter the linear density fluctuation field with a window of radius large enough so that $\sigma(R) = 1$ before applying the Zel'dovich approximation (the truncated Zel'dovich approximation of Kofman et al 1992). In both methods, coherent motion is reduced on small scales in virialized regions, which is in agreement with the fully nonlinear evolution of the gravitational potential (Melott et al 1996).

Sathyaprakash et al (1995) compared these modified Zel'dovich approximations and other dynamical approximations against *N*-body simulations, finding that the truncated Zel'dovich approximation is favored because of its simplicity and accuracy. Besides being slower, the adhesion approximation does not conserve comoving momentum. Shandarin & Sathyaprakash (1996) presented a promising new fast approximation that conserves momentum by replacing the Burgers equation of the adhesion approximation with the Navier-Stokes equation of viscous fluid flow.

The Zel'dovich approximation may be regarded as the first-order perturbation theory for the trajectories of mass elements. Higher-order Lagrangian perturbation theory would include additional terms in a power series in D in Equation 6. The second-order perturbation theory has been applied and compared against simulations of hierarchical models by Melott et al (1995) and Bouchet et al (1995), who concluded that it gives significant improvements over the Zel'dovich approximation, particularly when the initial density field is smoothed (truncated) at high wavenumbers. Karakatsanis et al (1997) have improved these methods further by artificially slowing down the growth of $D(t)$ in the perturbation series to prevent the displacements from growing too rapidly.

The least-action principle provides an alternative formulation of gravitational dynamics that underlies several new approximations. Peebles (1989, 1994; see also Giavalisco et al 1993) introduced the least-action method as a way to trace galaxy orbits back in time, given the final positions and requiring that the peculiar velocities vanish initially. By requiring the final velocities to match observations, the mean mass-to-light ratios of the galaxies can be deduced and, from this, Ω (Shaya et al 1995). Although simulations have raised questions about the reliability of this estimate (Branchini & Carlberg 1994, Dunn & Laflamme 1995), the least-action principle offers a powerful approach to dynamical approximations. Its difficulty lies in being nonlocal: The motion of all mass elements must be considered simultaneously to minimize the action. Its advantage over other techniques lies in the ability to reconstruct the initial conditions. Two impressive implementations of this idea have been published recently. Susperregi & Binney (1994) worked with Eulerian density and velocity

fields, whereas Croft & Gaztañaga (1997) used straight-line Lagrangian trajectories. Their methods agree reasonably well with *N*-body simulations and offer the hope that, with data from large redshift surveys, similar methods may allow accurate reconstruction of the initial density fluctuation field.

6. FUTURE DIRECTIONS

Ten years ago, the field of computational cosmology was in something of a doldrums, with the standard CDM model reeling and rather little to replace it. The experience brought valuable lessons to the field and encouraged new ideas and applications. Now simulations are used to provide invaluable insight into physical systems such as quasar absorption lines, despite our lack of a definite structure formation model.

During the next decade, simulations will be applied toward investigation of the leading outstanding questions in cosmology, such as the following. What are the values of the cosmological parameters? What is the dark matter and how much is there? What was the nature of the primordial density fluctuations? How different are the galaxy and mass density fields? When did galaxies and clusters of galaxies form? Why is galaxy morphology different in rich clusters from lower-density environments? What are the best ways to analyze the new large redshift surveys and other datasets that will become available?

Addressing many of these questions more rigorously than heretofore will require more physics and higher resolution than are available in current-generation simulations. Significant steps have been taken already with inclusion of multispecies chemistry in several gas dynamics codes. Improved treatments of radiative transfer and energy feedback through star formation will be required. In some environments, e.g. clusters of galaxies, inclusion of magnetic fields may be desirable. Yet for many problems, the limiting factor remains resolution. Gradually, this limitation will recede with the combination of adaptive algorithms and the relentless speedup of computers. Students wishing to enter this field will benefit from a broad background in physical processes, numerical algorithms, and high-performance computing in addition to astrophysics and cosmology.

ACKNOWLEDGMENTS

I gratefully acknowledge support from the National Science Foundation under grants AST-9318185 and AST-9529154 and from the National Aeronautics and Space Administration under grant NAG5-2816.

Literature Cited

Aarseth SJ. 1963. *MNRAS* 126:223–55
Aarseth SJ, Gott JR, Turner EL. 1979. *Ap. J.* 228:664–83
Abel T, Anninos P, Zhang Y, Norman ML. 1997. *New Astron.* 2:181–207
Albrecht A, Stebbins A. 1992a. *Phys. Rev. Lett.* 68:2121–24
Albrecht A, Stebbins A. 1992b. *Phys. Rev. Lett.* 69:2615–18
Allen B, Shellard EPS. 1990. *Phys. Rev. Lett.* 64:119–22
Anninos P, Norman ML. 1996. *Ap. J.* 459:12–26
Anninos P, Norman ML, Clarke DA. 1994. *Ap. J.* 436:11–22
Anninos P, Zhang Y, Abel T, Norman ML. 1997. *New Astron.* 2:209–24
Anninos WY, Norman ML. 1994. *Ap. J.* 429: 434–64
Appel AW. 1985. *SIAM J. Sci. Stat. Comp.* 6:85–93
Avelino PP. 1997. *Ap. J.* 487:18–32
Bahcall NA, Cen R. 1992. *Ap. J. Lett.* 398:L81–84
Bahcall NA, Cen R. 1993. *Ap. J. Lett.* 407:L49–52
Bahcall NA, Cen R, Gramann M. 1993. *Ap. J. Lett.* 408:L77–80
Bahcall NA, Lubin LM. 1994. *Ap. J.* 426:513–15
Balsara DS. 1995. *J. Comp. Phys.* 121:357–72
Bardeen JM, Bond JR, Kaiser N, Szalay AS. 1986. *Ap. J.* 304:15–61
Barnes J, Efstathiou G. 1987. *Ap. J.* 319:575–600
Barnes J, Hut P. 1986. *Nature* 324:446–49
Barnes J, Hut P. 1989. *Ap. J. Suppl.* 70:389–417
Bartelmann M. 1995. *Astron. Astrophys.* 303: 643–55
Bartelmann M, Narayan R, Seitz S, Schneider P. 1996. *Ap. J. Lett.* 464:L115–18
Bartelmann M, Steinmetz M. 1996. *MNRAS* 283:431–46
Bartelmann M, Steinmetz M, Weiss A. 1995. *Astron. Astrophys.* 297:1–12
Bate MR, Burkert A. 1997. *MNRAS* 288:1060–72
Baugh CM, Efstathiou G. 1994. *MNRAS* 270: 183–98
Baugh CM, Gaztañaga E. 1996. *MNRAS* 280: L37–41
Baugh CM, Gaztañaga E, Efstathiou G. 1995. *MNRAS* 274:1049–70
Beaky MM, Scherrer RJ, Villumsen JV. 1992. *Ap. J.* 387:443–48
Bennett DP, Bouchet FR. 1990. *Phys. Rev. D* 41:2408–33
Bernardeau F. 1994. *Astron. Astrophys.* 291: 697–712
Bernardeau F, Juszkiewicz R, Dekel A, Bouchet FR. 1995. *MNRAS* 274:20–26
Bernardeau F, Kofman L. 1995. *Ap. J.* 443:479–98
Bernardeau F, van de Weygaert R, Hivon E, Bouchet FR. 1997. *MNRAS* 290:566–76
Bertschinger E. 1987. *Ap. J. Lett.* 323:L103–6
Bertschinger E. 1992. In *New Insights into the Universe*, ed. VJ Martínez, M Portilla, D Sáez, pp. 64–126. New York: Springer-Verlag
Bertschinger E, Dekel A. 1989. *Ap. J. Lett.* 336: L5–8
Bertschinger E, Gelb JM. 1991. *Comp. Phys.* 5: 164–79
Bertschinger E, Juszkiewicz R. 1988. *Ap. J. Lett.* 334:L59–62
Bhavsar SP, Aarseth SJ, Gott JR. 1981. *Ap. J.* 246:656–65
Bhavsar SP, Barrow JD. 1983. *MNRAS* 205: 61p–66p
Bhavsar SP, Splinter RJ. 1996. *MNRAS* 282: 1461–66
Bi H, Davidsen AF. 1997. *Ap. J.* 479:523–42
Bi H, Ge J, Fang L-Z. 1995. *Ap. J.* 452:90–101
Binney J, Quinn T. 1991. *MNRAS* 249:678–83
Blandford RD, Narayan R. 1992. *Annu. Rev. Astron. Atrophys.* 30:311–58
Blumenthal GR, Faber SM, Flores R, Primack JR. 1986. *Ap. J.* 301:27–34
Blumenthal GR, Faber SM, Primack JR, Rees MJ. 1984. *Nature* 311:517–25
Bond JR. 1996. In *Cosmology and Large Scale Structure, Les Houches Session LX*, ed. R Schaeffer, J Silk, M Spiro, J Zinn-Justin, pp. 469–674. Amsterdam: Elsevier Sci.
Bond JR, Centrella J, Szalay AS, Wilson JR. 1984. *MNRAS* 210:515–45
Bond JR, Efstathiou G, Silk J. 1980. *Phys. Rev. Lett.* 45:1980–84
Bond JR, Kofman L, Pogosyan D. 1996. *Nature* 380:603–6
Bond JR, Szalay AS. 1983. *Ap. J.* 274:443–68
Bond JR, Szalay AS, Silk J. 1988. *Ap. J.* 324: 627–38
Borgani S, Moscardini L, Plionis M, Górski KM, Holtzman J, et al. 1997. *New Astron.* 1:321–47
Bouchet FR, Adam J-C, Pellat R. 1985. *Astron. Astrophys.* 144:413–26
Bouchet FR, Colombi S, Hivon E, Juszkiewicz R. 1995. *Astron. Astrophys.* 296:575–608
Bouchet FR, Hernquist L. 1988. *Ap. J. Suppl.* 68:521–38
Bouchet FR, Hernquist L. 1992. *Ap. J.* 400:25–40
Bouchet FR, Kandrup HE. 1985. *Ap. J.* 299:1–4

Bouchet FR, Schaeffer R, Davis M. 1991. *Ap. J.* 383:19–40
Brainerd TG, Bromley BC, Warren MS, Zurek WH. 1996. *Ap. J. Lett.* 464:L103–6
Brainerd TG, Villumsen JV. 1992. *Ap. J.* 394: 409–21
Brainerd TG, Villumsen JV. 1994a. *Ap. J.* 431: 477–85
Brainerd TG, Villumsen JV. 1994b. *Ap. J.* 436: 528–41
Branchini E, Carlberg RG. 1994. *Ap. J.* 434:37–45
Brandenberger R. 1994. *Int. J. Mod. Phys. A* 9:2117–89
Brieu PP, Summers FJ, Ostriker JP. 1995. *Ap. J.* 453:566–73
Bromley BC. 1994. *Ap. J.* 437:541–49
Bryan G, Norman M, Stone J, Cen R, Ostriker J. 1995. *Comp. Phys. Commun.* 89:149–68
Bryan GL, Klypin A, Loken C, Norman ML, Burns O. 1994. *Ap. J. Lett.* 437:L5–8
Bunn EF, White M. 1997. *Ap. J.* 480:6–21
Buote DA, Tsai JC. 1995. *Ap. J.* 452:522–37
Buote DA, Xu G. 1997. *MNRAS* 284:439–56
Carlberg RG. 1988a. *Ap. J.* 324:664–76
Carlberg RG. 1988b. *Ap. J.* 332:26–43
Carlberg RG. 1994. *Ap. J.* 433:468–78
Carlberg RG, Couchman HMP. 1989. *Ap. J.* 340:47–68
Carlberg RG, Couchman HMP, Thomas PA. 1990. *Ap. J. Lett.* 352:L29–32
Carroll SM, Press WH, Turner EL. 1992. *Annu. Rev. Astron. Atrophys.* 30:499–542
Cen R. 1992. *Ap. J. Suppl.* 78:341–64
Cen R. 1997a. *Ap. J.* 485:39–79
Cen R. 1997b. *Ap. J.* 491:1–5
Cen R, Gnedin NY, Kofman LA, Ostriker JP. 1992. *Ap. J. Lett.* 399: L11–14
Cen R, Gnedin NY, Ostriker JP. 1993a. *Ap. J.* 417:387–403
Cen R, Gott JR, Ostriker JP, Turner EL. 1994a. *Ap. J.* 423:1–11
Cen R, Miralda-Escudé J, Ostriker JP, Rauch M. 1994b. *Ap. J. Lett.* 437:L9–12
Cen R, Ostriker JP. 1992a. *Ap. J. Lett.* 399: L113–16
Cen R, Ostriker JP. 1992b. *Ap. J.* 399:331–44
Cen R, Ostriker JP. 1993a. *Ap. J.* 414:407–20
Cen R, Ostriker JP. 1993b. *Ap. J.* 417:404–14
Cen R, Ostriker JP. 1993c. *Ap. J.* 417:415–26
Cen R, Ostriker JP. 1994a. *Ap. J.* 429:4–21
Cen R, Ostriker JP. 1994b. *Ap. J.* 431:451–76
Cen R, Ostriker JP, Peebles PJE. 1993b. *Ap. J.* 415:423–44
Cen R, Simcoe RA. 1997. *Ap. J.* 483:8–20
Cen RY, Jameson A, Liu F, Ostriker JP. 1990. *Ap. J. Lett.* 362:L41–45
Cen RY, Ostriker JP, Spergel DN, Turok N. 1991. *Ap. J.* 383:1–18
Centrella J, Melott AL. 1983. *Nature* 305:196–98
Charlton JC, Anninos P, Zhang Y, Norman ML. 1997. *Ap. J.* 485:26–38
Chiang W-H, Ryu D, Vishniac ET. 1989. *Ap. J.* 339:603–18
Cole S. 1997. *MNRAS* 286:38–47
Cole S, Fisher KB, Weinberg DH. 1994. *MNRAS* 267:785–99
Cole S, Fisher KB, Weinberg DH. 1995. *MNRAS* 275:515–26
Cole S, Lacey C. 1996. *MNRAS* 281:716–36
Cole S, Weinberg DH, Frenk CS, Ratra B. 1997. *MNRAS* 289:37–51
Coles P. 1992. In *Statistical Challenges in Modern Astronomy*, ed. ED Feigelson, GJ Babu, pp. 57–81. New York: Springer
Coles P. 1993. *MNRAS* 262:1065–75
Coles P, Davies AG, Pearson RC. 1996. *MNRAS* 281:1375–84
Coles P, Ellis GFR. 1994. *Nature* 370:609–15
Coles P, Frenk CS. 1991. *MNRAS* 253:727–37
Coles P, Jones BJT. 1991. *MNRAS* 248:1–13
Coles P, Moscardini L, Lucchin F, Matarrese S, Messina A. 1993. *MNRAS* 264:749–57
Colin P, Carlberg RG, Couchman HMP. 1997. *Ap. J.* 490:1–10
Collela P, Woodward PR. 1984. *J. Comp. Phys.* 54:174–201
Colombi S, Bouchet FR, Hernquist L. 1996a. *Ap. J.* 465:14–33
Colombi S, Bouchet FR, Schaeffer R. 1992. *Astron. Astrophys.* 263:1–22
Colombi S, Bouchet FR, Schaeffer R. 1995. *Ap. J. Suppl.* 96:401–28
Colombi S, Dodelson S, Widrow LM. 1996b. *Ap. J.* 458:1–17
Cooley JW, Tukey JW. 1965. *Math. Comp.* 19:297–301
Copi CJ, Schramm DN, Turner MS. 1995. *Science* 267:192–99
Couchman HMP. 1991. *Ap. J. Lett.* 368:L23–26
Couchman HMP, Carlberg RG. 1992. *Ap. J.* 389:453–63
Couchman HMP, Rees MJ. 1986. *MNRAS* 221:53–62
Couchman HMP, Thomas PA, Pearce FR. 1995. *Ap. J.* 452:797–813
Cowsik R, McClelland J. 1972. *Phys. Rev. Lett.* 29:669–70
Croft RAC, Gaztañaga E. 1997. *MNRAS* 285:793–805
Croft RAC, Weinberg DH, Katz N, Hernquist L. 1997. *Ap. J.* 488:532–49
Crone MM, Evrard AE, Richstone DO. 1994. *Ap. J.* 434:402–16
Crone MM, Evrard AE, Richstone DO. 1996. *Ap. J.* 467:489–503
Davé R, Dubinski J, Hernquist L. 1997a. *New Astron.* 2:277–97
Davé R, Hellinger D, Primack J, Nolthenius R, Klypin A. 1997b. *MNRAS* 284:607–26

Davé R, Hernquist L, Weinberg DH, Katz N. 1997c. *Ap. J.* 477:21–26
Davies G, Widrow L. 1997. *Ap. J.* 485:484–95
Davis M, Efstathiou G, Frenk CS, White SDM. 1985. *Ap. J.* 292:371–94
Davis M, Efstathiou G, Frenk CS, White SDM. 1992a. *Nature* 356:489–94
Davis M, Miller A, White SDM. 1997. *Ap. J.* 490:63–71
Davis M, Peebles PJE. 1977. *Ap. J. Suppl.* 34: 425–50
Davis M, Peebles PJE. 1983. *Ap. J.* 267:465–82
Davis M, Summers FJ, Schlegel D. 1992b. *Nature* 359:393–96
Dekel A. 1982. *Ap. J. Lett.* 261:L13–17
Dekel A. 1994. *Annu. Rev. Astron. Atrophys.* 32:371–418
Dekel A, Rees MJ. 1987. *Nature* 326:455–62
Dekel A, Silk J. 1986. *Ap. J.* 303:39–55
Dekel A, West MJ. 1985. *Ap. J.* 288:411–17
Dodelson S, Gates EI, Turner MS. 1996. *Science* 274:69–75
Dominik KG, Shandarin SF. 1992. *Ap. J.* 393:450–63
Doroshkevich AG. 1970. *Astrophysica* 6:320–30
Doroshkevich AG, Kotok EV, Novikov ID, Polyudov AN, Shandarin SF, Sigov YuS. 1980. *MNRAS* 192:321–27
Doroshkevich AG, Shandarin SF, Saar E. 1978. *MNRAS* 184:643–60
Dubinski J. 1996. *New Astron.* 1:133–47
Dubinski J, Carlberg R. 1991. *Ap. J.* 378:496–503
Ducloux E, Leorat J, Gerbal D, Alecian G. 1992. *Astron. Astrophys.* 257:425–33
Dunn AM, Laflamme R. 1995. *Ap. J. Lett.* 443:L1–4
Dutta SN. 1995. *MNRAS* 276:1109–15
Efstathiou G. 1979. *MNRAS* 189:203–20
Efstathiou G. 1992. *MNRAS* 256:43p–47p
Efstathiou G. 1996. In *Cosmology and Large Scale Structure, Les Houches Session LX*, ed. R Schaeffer, J Silk, M Spiro, J Zinn-Justin, pp. 133–252. Amsterdam: Elsevier Sci.
Efstathiou G, Bond JR, White SDM. 1992. *MNRAS* 258:1p–6p
Efstathiou G, Davis M, Frenk CS, White SDM. 1985. *Ap. J. Suppl.* 57:241–60
Efstathiou G, Eastwood JW. 1981. *MNRAS* 194:503–25
Efstathiou G, Fall SM, Hogan C. 1979. *MNRAS* 189:203–20
Efstathiou G, Frenk CS, White SDM, Davis M. 1988. *MNRAS* 235:715–48
Efstathiou G, Sutherland WJ, Maddox SJ. 1990. *Nature* 348:705–7
Einasto J, Einasto M, Gramann M, Saar M. 1991. *MNRAS* 248:593–605
Eke VR, Cole S, Frenk CS. 1996. *MNRAS* 282: 263–80
Evans NW, Collett JL. 1997. *Ap. J. Lett.* 480: L103–6
Evrard AE. 1988. *MNRAS* 235:911–34
Evrard AE. 1989. *Ap. J. Lett.* 341:L71–74
Evrard AE. 1990. *Ap. J.* 363:349–66
Evrard AE. 1997. *MNRAS* 292:289–97
Evrard AE, Metzler CA, Navarro JF. 1996. *Ap. J.* 469:494–507
Evrard AE, Mohr JJ, Fabricant DG, Geller M. 1993. *Ap. J. Lett.* 419:L9–12
Evrard AE, Summers FJ, Davis M. 1994. *Ap. J.* 422:11–36
Ewald PP. 1921. *Ann. Phys.* 64:253–87
Faber SM, Tremaine S, Ajhar EA, Byun Y-I, Dressler A, et al. 1997. *Astron. J.* 114:1771–96
Fall SM. 1978. *MNRAS* 185:165–77
Fan X, Bahcall NA, Cen R. 1997. *Ap. J. Lett.* 490:L123–26
Ferland GJ, Korista KT, Verner DA, Ferguson JW, Kingdon JB, Verner EM. 1998. *Publ. Astron. Soc. Pac.* 110(749):In press
Ferrell R, Bertschinger E. 1994. *Int. J. Mod. Phys. C* 5:933–56
Ferrell R, Bertschinger E. 1995. In *High Performance Computing 1995, Grand Challenges in Computer Simulation*, ed. A Tentner, pp. 88–94. San Diego: Soc. Comput. Simul.
Fillmore JA, Goldreich P. 1984. *Ap. J.* 281:1–8
Frenk CS. 1991. *Phys. Scr.* T36:70–87
Frenk CS, Evrard AE, White SDM, Summers FJ. 1996. *Ap. J.* 472:460–84
Frenk CS, White SDM, Davis M, Efstathiou G. 1988. *Ap. J.* 327:507–25
Frenk CS, White SDM, Efstathiou G, Davis M. 1985. *Nature* 317:595–97
Fry JN, Melott AL, Shandarin SF. 1993. *Ap. J.* 412:504–12
Fukushige T, Makino J. 1997. *Ap. J. Lett.* 477: L9–12
Fukushige T, Taiji M, Makino J, Ebisuzaki T, Sugimoto D. 1996. *Ap. J.* 468:51–61
Ganon G, Hoffman Y. 1993. *Ap. J. Lett.* 415:L5–8
Gardner JP, Katz N, Weinberg DH, Hernquist L. 1997. *Ap. J.* 486:42–47
Gelato S, Chernoff DF, Wasserman I. 1997. *Ap. J.* 480:115–31
Gelb JM, Bertschinger E. 1994a. *Ap. J.* 436: 467–90
Gelb JM, Bertschinger E. 1994b. *Ap. J.* 436: 491–508
Gelb JM, Gradwohl B-A, Frieman JA. 1993. *Ap. J. Lett.* 403:L5–8
Giavalisco M, Mancinelli B, Mancinelli PJ, Yahil A. 1993. *Ap. J.* 411:9–15
Gingold RA, Monaghan JJ. 1977. *MNRAS* 181:375–89
Gnedin NY. 1995. *Ap. J. Suppl.* 97:231–57
Gnedin NY. 1996a. *Ap. J.* 456:1–33

Gnedin NY. 1996b. *Ap. J.* 456:34–42
Gnedin NY, Bertschinger E. 1996. *Ap. J.* 470:115–30
Gnedin NY, Hui L. 1996. *Ap. J. Lett.* 472:L73–76
Gnedin NY, Ostriker JP. 1997. *Ap. J.* 486:581–98
Gooding AK, Park C, Spergel DN, Turok N, Gott JR. 1992. *Ap. J.* 393:42–58
Goodman J, Heggie DC, Hut P. 1993. *Ap. J.* 415:715–33
Gott JR. 1977. *Annu. Rev. Astron. Atrophys.* 15:235–66
Gott JR, Melott AL, Dickinson M. 1986. *Ap. J.* 306:341–57
Gott JR, Turner EL, Aarseth SJ. 1979. *Ap. J.* 234:13–26
Gouda N. 1994. *Ap. J.* 436:542–46
Governato F, Moore B, Cen R, Stadel J, Lake G, Quinn T. 1997. *New Astron.* 2:91–106
Gramann M, Cen R, Gott JR. 1994. *Ap. J.* 425:382–91
Gramann M, Einasto J. 1992. *MNRAS* 254:453–65
Greengard L, Rokhlin V. 1987. *J. Comp. Phys.* 73:325–48
Groth EJ, Peebles PJE. 1976. *Astron. Astrophys.* 53:131–40
Groth EJ, Peebles PJE. 1977. *Ap. J.* 217:385–405
Gunn JE, Gott JR. 1972. *Ap. J.* 176:1–19
Gunn JE, Peterson BA. 1965. *Ap. J.* 142:1633–36
Gurbatov SN, Saichev AI, Shandarin SF. 1989. *MNRAS* 236:385–402
Guth AH. 1981. *Phys. Rev. D* 23:347–56
Guth AH, Pi S-Y. 1985. *Phys. Rev. D* 32:1899–920
Haehnelt MG, Rauch M, Steinmetz M. 1996a. *MNRAS* 283:1055–60
Haehnelt MG, Steinmetz M, Rauch M. 1996b. *Ap. J. Lett.* 465:L95–98
Haggerty MJ, Janin G. 1974. *Astron. Astrophys.* 36:415–27
Haiman Z, Thoul AA, Loeb A. 1996. *Ap. J.* 464:523–38
Hamilton AJS. 1993. *Ap. J.* 417:19–35
Hamilton AJS, Gott JR, Weinberg D. 1986. *Ap. J.* 309:1–12
Hamilton AJS, Kumar P, Lu E, Matthews A. 1991. *Ap. J. Lett.* 374:L1–4
Harrison ER. 1970. *Phys. Rev. D* 1:2726–30
Hellsten U, Davé R, Hernquist L, Weinberg DH, Katz N. 1997. *Ap. J.* 487:482–88
Hernquist L. 1987. *Ap. J. Suppl.* 64:715–34
Hernquist L. 1988. *Comp. Phys. Commun.* 48:107–15
Hernquist L. 1990. *Ap. J.* 356:359–64
Hernquist L. 1993. *Ap. J.* 404:717–22
Hernquist L, Bouchet FR, Suto Y. 1991. *Ap. J. Suppl.* 75:231–40
Hernquist L, Hut P, Makino J. 1993. *Ap. J. Lett.* 402:L85–88
Hernquist L, Katz N. 1989. *Ap. J. Suppl.* 70:419–46
Hernquist L, Katz N, Weinberg DH, Miralda-Escudé J. 1996. *Ap. J. Lett.* 457:L51–55
Hillis WD, Barnes J. 1987. *Nature* 326:27–30
Hockney RW, Eastwood JW. 1988. *Computer Simulation Using Particles*. Bristol: Adam Hilger
Hockney RW, Goel SP, Eastwood JW. 1974. *J. Comp. Phys.* 14:148–58
Hoffman Y, Ribak E. 1991. *Ap. J. Lett.* 380:L5–8
Hoffman Y, Shaham J. 1985. *Ap. J.* 297:16–22
Hohl F, Hockney RW. 1969. *J. Comp. Phys.* 4:306–23
Holmberg E. 1941. *Ap. J.* 94:385–95
Holtzman J. 1989. *Ap. J. Suppl.* 71:1–24
Hozumi S. 1997. *Ap. J.* 487:617–24
Hu W, Bunn EF, Sugiyama N. 1995. *Ap. J. Lett.* 447:L59–63
Huang S, Dubinski J, Carlberg RG. 1993. *Ap. J.* 404:73–80
Hui L, Gnedin NY, Zhang Y. 1997. *Ap. J.* 486:599–622
Hut P, Makino J, McMillan S. 1995. *Ap. J. Lett.* 443:L93–96
Inagaki S, Itoh M, Saslaw WC. 1992. *Ap. J.* 386:9–18
Itoh M, Inagaki S, Saslaw WC. 1988. *Ap. J.* 331:45–63
Jain B. 1997. *MNRAS* 287:687–98
Jain B, Mo HJ, White SDM. 1995. *MNRAS* 276:L25–29
James RA. 1977. *J. Comp. Phys.* 25:71–93
Jameson A. 1989. *Science* 245:361–71
Jernigan JG, Porter DH. 1989. *Ap. J. Suppl.* 71:871–93
Jessop C, Duncan M, Chau WY. 1994. *J. Comp. Phys.* 115:339–51
Jing YP, Mo HJ, Börner G, Fang LZ. 1993. *Ap. J.* 411:450–54
Jones BJT, Martínez VJ, Saar A, Einasto J. 1988. *Ap. J. Lett.* 332:L1–5
Juszkiewicz R, Bouchet FR, Colombi S. 1993. *Ap. J. Lett.* 412:L9–12
Juszkiewicz R, Weinberg DH, Amsterdamski P, Chodorowski M, Bouchet F. 1995. *Ap. J.* 442:39–56
Kaiser N. 1984. *Ap. J. Lett.* 284:L9–12
Kaiser N. 1987. *MNRAS* 227:1–21
Kaiser N, Squires G. 1993. *Ap. J.* 404:441–50
Kang H, Ostriker JP, Cen R, Ryu D, Hernquist L, et al. 1994. *Ap. J.* 430:83–100
Karakatsanis G, Buchert T, Melott AL. 1997. *Astron. Astrophys.* 326:873–84
Katz N. 1992. *Ap. J.* 391:502–17
Katz N, Gunn JE. 1991. *Ap. J.* 377:365–81
Katz N, Quinn T, Bertschinger E, Gelb JM. 1994. *MNRAS* 270:L71–74

Katz N, Quinn T, Gelb JM. 1993. *MNRAS* 265:689–705
Katz N, Weinberg DH, Hernquist L. 1996a. *Ap. J. Suppl.* 105:19–35
Katz N, Weinberg DH, Hernquist L, Miralda-Escudé J. 1996b. *Ap. J. Lett.* 457:L57–60
Katz N, White SDM. 1993. *Ap. J.* 412:455–78
Kauffmann G, Nusser A, Steinmetz M. 1997. *MNRAS* 286:795–811
Kauffmann G, White SDM. 1992. *MNRAS* 258:511–20
Kepner JV, Babul A, Spergel DN. 1997a. *Ap. J.* 487:61–68
Kepner JV, Summers FJ, Strauss MA. 1997b. *New Astron.* 2:165–80
Klypin A, Borgani S, Holtzman J, Primack J. 1995. *Ap. J.* 444:1–14
Klypin A, Holtzman J, Primack J, Regös E. 1993. *Ap. J.* 416:1–16
Klypin A, Primack J, Holtzman J. 1996. *Ap. J.* 466:13–20
Klypin AA, Shandarin SF. 1983. *MNRAS* 204:891–907
Kofman L, Bertschinger E, Gelb JM, Nusser A, Dekel A. 1994. *Ap. J.* 420:44–57
Kofman L, Pogosyan D, Shandarin SF, Melott AL. 1992. *Ap. J.* 393:437–49
Kravtsov AV, Klypin AA, Khokhlov AM. 1997. *Ap. J. Suppl.* 111:73–94
Krzewina LG, Saslaw WC. 1996. *MNRAS* 278:869–76
Lacey C, Cole S. 1994. *MNRAS* 271:676–92
Landau LD, Liftshitz EM. 1959. *Fluid Mechanics.* Oxford: Pergamon
Larson RB. 1969. *MNRAS* 145:405–22
Lee BW, Weinberg S. 1977. *Phys. Rev. Lett.* 39:165–68
LeVeque RJ. 1992. *Numerical Methods for Conservation Laws.* Boston: Birkhauser
Liddle AR, Lyth DH. 1993. *Phys. Rep.* 231:1–105
Liddle AR, Lyth DH, Roberts D, Viana PTP. 1996a. *MNRAS* 278:644–54
Liddle AR, Lyth DH, Schaefer RK, Shafi Q, Viana PTP. 1996b. *MNRAS* 281:531–51
Liddle AR, Lyth DH, Viana PTP, White M. 1996c. *MNRAS* 282:281–90
Little B, Weinberg DH, Park C. 1991. *MNRAS* 253:295–306
Lokas EL, Juszkiewicz R, Weinberg DH, Bouchet FR. 1995. *MNRAS* 274:730–44
Lucy LB. 1977. *Astron. J.* 82:1013–24
Luo S, Vishniac ET. 1995. *Ap. J.* 443:469–78
Lynden-Bell D, Faber SM, Burstein D, Davies RL, Dressler A, et al. 1988. *Ap. J.* 326:19–49
Ma C-P. 1996. *Ap. J.* 471:13–23
Ma C-P, Bertschinger E. 1994a. *Ap. J.* 429:22–28
Ma C-P, Bertschinger E. 1994b. *Ap. J. Lett.* 434:L5–9
Ma C-P, Bertschinger E. 1995. *Ap. J.* 455:7–25
Maddox SJ, Efstathiou G, Sutherland WJ, Loveday J. 1990. *MNRAS* 242:43p–47p
Makino J, Hut P. 1989. *Comp. Phys. Rep.* 9:199–246
Makino J, Taiji M, Ebisuzaki T, Sugimoto D. 1997. *Ap. J.* 480:432–46
Martel H. 1991. *Ap. J.* 366:353–83
Martínez VJ, Jones BJT, Domínguez-Tenreiro R, van de Weygaert R. 1990. *Ap. J.* 357:50–61
Matsubara T. 1994. *Ap. J.* 424:30–41
Matsubara T. 1996. *Ap. J.* 457:13–18
Matsubara T, Yokoyama J. 1996. *Ap. J.* 463:409–19
McGill C. 1990. *MNRAS* 242:544–54
Mecke KB, Buchert T, Wagner H. 1994. *Astron. Astrophys.* 288:697–704
Melott AL. 1982. *Phys. Rev. Lett.* 48:894–96
Melott AL. 1983. *MNRAS* 202:595–604
Melott AL. 1990. *Phys. Rep.* 193:1–39
Melott AL, Buchert T, Weiss AG. 1995. *Astron. Astrophys.* 294:345–65
Melott AL, Sathyaprakash BS, Sahni V. 1996. *Ap. J.* 456:65–70
Melott AL, Shandarin SF. 1989. *Ap. J.* 343:26–30
Melott AL, Shandarin SF, Splinter RJ, Suto Y. 1997. *Ap. J. Lett.* 479:L79–83
Mihos JC, Hernquist L. 1994. *Ap. J.* 437:611–24
Miller RH. 1970. *J. Comp. Phys.* 6:449–72
Miller RH. 1983. *Ap. J.* 270:390–409
Miller RH, Prendergast KM. 1968. *Ap. J.* 151:699–709
Miralda-Escudé J, Cen R, Ostriker JP, Rauch M. 1996. *Ap. J.* 471:582–616
Miyoshi K, Kihara T. 1975. *Publ. Astron. Soc. Jpn.* 27:333–46
Mo HJ, Jing YP, Börner G. 1992. *Ap. J.* 392:452–57
Mo HJ, Jing YP, White SDM. 1996. *MNRAS* 282:1096–104
Mo HJ, White SDM. 1996. *MNRAS* 282:347–61
Monaghan JJ. 1992. *Annu. Rev. Astron. Astrophys.* 30:543–74
Moore B, Katz N, Lake G. 1996. *Ap. J.* 457:455–59
Moscardini L, Matarrese S, Lucchin F, Messina A. 1991. *MNRAS* 248:424–38
Moscardini L, Tormen G, Matarrese S, Lucchin F. 1995. *Ap. J.* 442:469–79
Mücket JP, Petitjean P, Kates R, Riediger R. 1996. *Astron. Astrophys.* 308:17–26
Nakasato N, Mori M, Nomoto K. 1997. *Ap. J.* 484:608–17
Narayan R, White SDM. 1988. *MNRAS* 231:97p–103p
Navarro JF, Frenk CS, White SDM. 1995. *MNRAS* 275:720–40
Navarro JF, Frenk CS, White SDM. 1996. *Ap. J.* 462:563–75

Navarro JF, Frenk CS, White SDM. 1997. *Ap. J.* 490:493–508
Navarro JF, Steinmetz M. 1997. *Ap. J.* 478:13–28
Navarro JF, White SDM. 1993. *MNRAS* 265: 271–300
Olson KM, Dorbrand JE. 1994. *Ap. J. Suppl.* 94:117–25
Ostriker JP. 1993. *Annu. Rev. Astron. Atrophys.* 31:689–716
Ostriker JP, Gnedin NY. 1996. *Ap. J. Lett.* 472: L63–67
Ostriker JP, Steinhardt PJ. 1995. *Nature* 377: 600–2
Ostriker JP, Suto Y. 1990. *Ap. J.* 348:378–82
Owen JM, Villumsen JV. 1997. *Ap. J.* 481:1–21
Padmanabhan T. 1996. *MNRAS* 278:L29–33
Padmanabhan T, Cen R, Ostriker JP, Summers FJ. 1996. *Ap. J.* 466:604–13
Park C. 1991. *MNRAS* 251:167–73
Park C, Gott JR. 1991. *Ap. J.* 378:457–60
Park C, Spergel DN, Turok N. 1991. *Ap. J. Lett.* 372:L53–57
Peacock JA. 1997. *MNRAS* 284:885–98
Peacock JA, Dodds SJ. 1994. *MNRAS* 267: 1020–34
Peacock JA, Dodds SJ. 1996. *MNRAS* 280:L19–26
Peacock JA, Heavens AF. 1985. *MNRAS* 217: 805–20
Pearce FR, Couchman HMP. 1997. *New Astron.* 2:411–27
Pearson RC, Coles P. 1995. *MNRAS* 272:231–40
Peebles PJE. 1970. *Astron. J.* 75:13–20
Peebles PJE. 1974. *Ap. J. Lett.* 189:L51–53
Peebles PJE. 1980. *The Large-Scale Structure of the Universe*. Princeton: Princeton Univ. Press
Peebles PJE. 1982. *Ap. J. Lett.* 263:L1–5
Peebles PJE. 1985. *Ap. J.* 297:350–60
Peebles PJE. 1986. *Nature* 321:27–32
Peebles PJE. 1987a. *Ap. J. Lett.* 315:L73–76
Peebles PJE. 1987b. *Ap. J.* 317:576–87
Peebles PJE. 1989. *Ap. J. Lett.* 344:L53–56
Peebles PJE. 1993. *Principles of Physical Cosmology*. Princeton: Princeton Univ. Press
Peebles PJE. 1994. *Ap. J.* 429:43–65
Peebles PJE, Daly RA, Juszkiewicz R. 1989. *Ap. J.* 347:563–74
Peebles PJE, Dicke RH. 1968. *Ap. J.* 154:891–908
Peebles PJE, Yu JT. 1970. *Ap. J.* 162:815–36
Pen U-L. 1995. *Ap. J. Suppl.* 100:269–80
Pen U-L. 1997. *Ap. J. Lett.* 490:L127–30
Pen U-L, Seljak U, Turok N. 1997. *Phys. Rev. Lett.* 79:1611–14
Pinkney J, Roettiger K, Burns JO, Bird CM. 1996. *Ap. J. Suppl.* 104:1–36
Press WH, Schechter PL. 1974. *Ap. J.* 187:425–38
Protogeros ZAM, Melott AL, Scherrer RJ. 1997. *MNRAS* 290:367–70
Protogeros ZAM, Scherrer RJ. 1997. *MNRAS* 284:425–38
Quilis V, Ibañez JM, Sáez D. 1994. *Astron. Astrophys.* 286:1–16
Quilis V, Ibañez JM, Sáez D. 1996. *Ap. J.* 469:11–25
Quinn PJ, Salmon JK, Zurek WH. 1986. *Nature* 322:329–35
Quinn T, Katz N, Staedel J, Lake G. 1997. *Ap. J.* Submitted (astro-ph/9710043)
Rauch M. 1998. *Annu. Rev. Astron. Atrophys.* 36:267–316
Rauch M, Haehnelt MG, Steinmetz M. 1997a. *Ap. J.* 481:601–24
Rauch M, Miralda-Escudé J, Sargent WLW, Barlow TA, Weinberg DH, et al. 1997b. *Ap. J.* 489:7–20
Raychaudhury S, Saslaw WC. 1996. *Ap. J.* 461: 514–24
Reisenegger A, Miralda-Escudé J. 1995. *Ap. J.* 449:476–87
Richstone D, Loeb A, Turner EL. 1992. *Ap. J.* 393:477–83
Richtmeyer RD, Morton KW. 1967. *Difference Methods for Initial-Value Problems.* New York: Wiley-Interscience.
Ruffa GJ, Porter DH. 1993. *Ap. J. Suppl.* 87: 179–95
Ryden BS. 1988. *Ap. J. Lett.* 333:L41–44
Ryden BS, Melott AL, Craig DA, Gott JR, Weinberg DH, et al. 1989. *Ap. J.* 340:647–60
Ryu D, Ostriker JP, Kang H, Cen R. 1993. *Ap. J.* 414:1–19
Ryu D, Vishniac ET, Chiang W-H. 1990. *Ap. J.* 354:389–99
Sahni V, Coles P. 1995. *Phys. Rep.* 262:1–136
Sahni V, Sathyaprakash BS, Shandarin SF. 1997. *Ap. J. Lett.* 476:L1–5
Salmon J. 1996. *Ap. J.* 460:59–67
Salmon J, Hogan C. 1986. *MNRAS* 221:93–104
Salmon JK, Warren MS. 1994. *J. Comp. Phys.* 111:136–55
Sanders RH, Prendergast KH. 1974. *Ap. J.* 188: 489–500
Saslaw WC, Hamilton AJS. 1984. *Ap. J.* 276: 13–25
Sathyaprakash BS, Sahni V, Munshi D, Pogosyan D, Melott AL. 1995. *MNRAS* 275:463–82
Saunders W, Frenk C, Rowan-Robinson M, Efstathiou G, Lawrence A, et al. 1991. *Nature* 349:32–38
Scherrer RJ, Melott AL, Bertschinger E. 1989. *Phys. Rev. Lett.* 62:379–82
Schmalzing J, Buchert T. 1997. *Ap. J. Lett.* 482:L1–4
Seljak U, Zaldarriaga M. 1996. *Ap. J.* 469:437–44

Sellwood JA. 1987. *Annu. Rev. Astron. Atrophys.* 25:151–86
Serna A, Alimi J-M, Chièze J-P. 1996. *Ap. J.* 461:884–96
Seto N, Yokoyama J, Matsubara T, Siino M. 1997. *Ap. J. Suppl.* 110:177–89
Shandarin SF, Sathyaprakash BS. 1996. *Ap. J. Lett.* 467:L25–28
Shandarin SF, Zel'dovich YaB. 1989. *Rev. Mod. Phys.* 61:185–220
Shapiro PR, Giroux ML. 1987. *Ap. J. Lett.* 321:L107–12
Shapiro PR, Kang H. 1987 *Ap. J.* 318:32–65
Shapiro PR, Martel H, Villumsen JV, Owen JM. 1996. *Ap. J. Suppl.* 103:269–330
Shapiro PR, Struck-Marcell C. 1985. *Ap. J. Suppl.* 57:205–39
Shapiro PR, Struck-Marcell C, Melott AL. 1983. *Ap. J.* 275:413–29
Shaya EJ, Peebles PJE, Tully RB. 1995. *Ap. J.* 454:15–31
Sheth RK. 1995. *MNRAS* 277:933–44
Sheth RK. 1996. *MNRAS* 279:1310–24
Sheth RK, Saslaw WC. 1996. *Ap. J.* 470:78–91
Shields JC, Ferland GJ. 1994. *Ap. J.* 430:236–51
Smoot GF, Bennett CL, Kogut A, Wright EL, Aymon J, et al. 1992. *Ap. J. Lett.* 396:L1–5
Sod GA. 1985. *Numerical Methods in Fluid Dynamics.* Cambridge: Cambridge Univ. Press
Somerville RS, Primack J, Nolthenius R. 1997. *Ap. J.* 479:606–15
Sornborger A, Brandenberger R, Fryxell B, Olson K. 1997. *Ap. J.* 482:22–32
Splinter RJ. 1996. *MNRAS* 281:281–93
Splinter RJ, Melott AL, Shandarin SF, Suto Y. 1998. *Ap. J.* 497:38–61
Steinhardt PJ. 1995. *Int. J. Mod. Phys. A* 10:1091–124
Steinmetz M. 1996. *MNRAS* 278:1005–17
Steinmetz M, Müller E. 1993. *Astron. Astrophys.* 268:391–410
Steinmetz M, White SDM. 1997. *MNRAS* 288: 545–50
Stone JM, Mihalas D, Norman ML. 1992. *Ap. J. Suppl.* 80:819–45
Stone JM, Norman ML. 1992. *Ap. J. Suppl.* 80:753–818
Strauss MA, Willick JA. 1995. *Phys. Rep.* 261: 271–431
Suginohara T, Suto Y. 1991. *Ap. J.* 371:470–77
Suginohara T, Suto Y. 1992a. *Ap. J.* 387:431–38
Suginohara T, Suto Y. 1992b. *Ap. J.* 396:395–410
Suisalu L, Saar E. 1995. *MNRAS* 274:287–99
Summers FJ, Davis M, Evrard AE. 1995. *Ap. J.* 454:1–14
Susperregi M, Binney J. 1994. *MNRAS* 271: 719–28
Suto Y, Itoh M, Inagaki S. 1990. *Ap. J.* 350:492–501
Suto Y, Suginohara T. 1991. *Ap. J. Lett.* 370: L15–18
Teyssier R, Chièze J-P, Alimi J-M. 1997. *Ap. J.* 480:36–42
Theuns T. 1994. *Comp. Phys. Commun.* 78: 238–46
Thomas PA, Couchman HMP. 1992. *MNRAS* 257:11–31
Tissera PB, Lambas DG, Abadi MG. 1994. *Ap. J.* 429:29–35
Tissera PB, Lambas DG, Abadi MG. 1997. *MNRAS* 286:384–92
Tormen G, Bertschinger E. 1996. *Ap. J.* 472:14–24
Tormen G, Bouchet FR, White SDM. 1997. *MNRAS* 286:865–84
Totsuji H, Kihara T. 1969. *Publ. Astron. Soc. Jpn.* 21:221–28
Trimble V. 1987. *Annu. Rev. Astron. Atrophys.* 25:425–72
Truelove JK, Klein RI, McKee CF, Holliman JH, Howell LH, Greenough JA. 1997. *Ap. J. Lett.* 489:L179–83
Tsai JC, Katz N, Bertschinger E. 1994. *Ap. J.* 423:553–65
Tytler D, Fan X-M, Burles S. 1996. *Nature* 381:207–9
Ueda H, Itoh M, Suto Y. 1993. *Publ. Astron. Soc. Jpn.* 45:7–23
Ueda H, Shimasaku K, Suginohara T, Suto Y. 1994. *Publ. Astron. Soc. Jpn.* 46:319–33
Ueda H, Yokoyama J. 1996. *MNRAS* 280:754–66
van de Weygaert R, Bertschinger E. 1996. *MNRAS* 281:84–118
Vilenkin A, Shellard EPS. 1994. *Cosmic Strings and Other Topological Defects*. Cambridge: Cambridge Univ. Press
Villumsen JV. 1989. *Ap. J. Suppl.* 71:407–31
Villumsen JV, Scherrer RJ, Bertschinger E. 1991. *Ap. J.* 367:37–44
Vishniac ET, Ostriker JP, Bertschinger E. 1985. *Ap. J.* 291:399–416
Vogeley MS, Park C, Geller MJ, Huchra JP. 1992. *Ap. J. Lett.* 391:L5–8
von Hoerner S. 1960. *Z. Astrophys.* 50:184–214
von Hoerner S. 1963. *Z. Astrophys.* 57:47–82
Wambsganss J, Cen R, Ostriker JP, Turner EL. 1995. *Science* 268:274–76
Warren MS, Quinn PJ, Salmon JK, Zurek WH. 1992. *Ap. J.* 399:405–25
Weinberg DH, Cole S. 1992. *MNRAS* 259:652–94
Weinberg DH, Hernquist L, Katz N. 1997a. *Ap. J.* 477:8–20
Weinberg DH, Miralda-Escudé J, Hernquist L, Katz N. 1997b. *Ap. J.* 490:564–70
White M, Scott D, Silk J. 1994. *Annu. Rev. Astron. Atrophys.* 32:319–70
White M, Scott D, Silk J, Davis M. 1995. *MNRAS* 276:L69–75

White SDM. 1976. *MNRAS* 177:717–33
White SDM. 1979. *MNRAS* 186:145–54
White SDM. 1996. In *Cosmology and Large Scale Structure, Les Houches Session LX*, ed. R Schaeffer, J Silk, M Spiro, J Zinn-Justin, pp. 349–430. Amsterdam: Elsevier Sci.
White SDM, Davis M, Efstathiou G, Frenk CS. 1987a. *Nature* 330:451–53
White SDM, Davis M, Frenk CS. 1984. *MNRAS* 209:27p–31p
White SDM, Efstathiou G, Frenk CS. 1993a. *MNRAS* 262:1023–28
White SDM, Frenk CS, Davis M. 1983. *Ap. J. Lett.* 274:L1–5
White SDM, Frenk CS, Davis M, Efstathiou G. 1987b. *Ap. J.* 313:505–16
White SDM, Navarro JF, Evrard AE, Frenk CS. 1993b. *Nature* 366:429–33
White SDM, Rees MJ. 1978. *MNRAS* 183:341–58
Widrow LM, Kaiser N. 1993. *Ap. J. Lett.* 416: L71–74
Wilson G, Cole S, Frenk CS. 1996a. *MNRAS* 280:199–218
Wilson G, Cole S, Frenk CS. 1996b. *MNRAS* 282:501–10
Woodward PR, Collela P. 1984. *J. Comp. Phys.* 54:115–73
Wright EL, Meyer SS, Bennett CL, Boggess NW, Cheng SS, et al. 1992. *Ap. J. Lett.* 396: L13–18
Xu G. 1995. *Ap. J. Suppl.* 98:355–66
Xu G. 1997. *MNRAS* 288:903–19
Yess C, Shandarin SF. 1996. *Ap. J.* 465:2–13
Yuan W, Centrella JM, Norman ML. 1991. *Ap. J. Lett.* 376:L29–32
Zaroubi S, Naim A, Hoffman Y. 1996. *Ap. J.* 457:50–60
Zel'dovich YaB. 1970. *Astron. Astrophys.* 5:84–89
Zel'dovich YaB. 1972. *MNRAS* 160:1p–3p
Zel'dovich YaB, Einasto J, Shandarin SF. 1982. *Nature* 300:407–13
Zhang Y, Anninos P, Norman ML. 1995. *Ap. J. Lett.* 453:L57–60
Zhang Y, Anninos P, Norman ML, Meiksin A. 1997. *Ap. J.* 485:496–516
Zurek WH, Quinn PJ, Salmon JK. 1988. *Ap. J.* 330:519–34
Zurek WH, Quinn PJ, Salmon JK, Warren MS. 1994. *Ap. J.* 431:559–68

Annual Review of Astronomy and Astrophysics
Volume 36, 1998

CONTENTS